Environment International 149 (2021) 106411

Contents lists available at ScienceDirect

Environment International

journal homepage: www.elsevier.com/locate/envint

The E-Morph Assay: Identification and characterization of environmental chemicals with estrogenic activity based on quantitative changes in cell-cell contact organization of breast cancer cells

Marja Kornhuber [a,b], Sebastian Dunst [a], Gilbert Schönfelder [a,c], Michael Oelgeschläger [a,*]

[a] German Federal Institute for Risk Assessment (BfR), German Centre for the Protection of Laboratory Animals (Bf3R), 10589 Berlin, Germany
[b] Freie Universität Berlin, 14195 Berlin, Germany
[c] Charité – Universitätsmedizin Berlin, Corporate Member of Freie Universität Berlin, Humboldt-Universität zu Berlin, and Berlin Institute of Health, 10117 Berlin, Germany

ARTICLE INFO

Handling Editor: Martí Nadal

Keywords:
Screening assays
Endocrine disruption
Estrogen
Adherens junction
Breast cancer

ABSTRACT

Adverse health effects that are caused by endocrine disrupting chemicals (EDCs) in the environment, food or consumer products are of high public concern. The identification and characterization of EDCs including substances with estrogenic activity still necessitates the use of animal testing as most of the approved alternative test methods only address single mechanistic events of endocrine activity. Therefore, novel human-relevant *in vitro* assays covering more complex functional endpoints of adversity, including hormone-related tumor formation and progression, are needed. This study describes the development and evaluation of a novel high-throughput screening-compatible assay called "E-Morph Assay". This image-based phenotypic screening assay facilitates robust predictions of the estrogenic potential of environmental chemicals using quantitative changes in the cell-cell contact morphology of human breast cancer cells as a novel functional endpoint. Based on a classification model, which was developed using six reference substances with known estrogenic activity, the E-Morph Assay correctly classified an additional set of 11 reference chemicals commonly used in OECD Test Guidelines and the U.S. EPA ToxCast program. For each of the tested substances, a relative ER bioactivity score was derived that allowed their grouping into four main categories of estrogenic activity, i.e. 'strong' (>0.9; four substances, i.e. natural hormones or pharmaceutical products), 'moderate' (0.9–0.6; six substances, i.e. phytoestrogens and Bisphenol AF), 'weak' (<0.6; three substances, i.e Bisphenol S, B, and A), and 'negative' (0.0; four substances). The E-Morph Assay considerably expands the portfolio of test methods providing the possibility to characterize the influence of environmental chemicals on estrogen-dependent tumor progression.

1. Introduction

The increasing scientific evidence describing detrimental human health effects caused by endocrine disrupting chemicals (EDCs) led to the development of dedicated governmental testing and screening frameworks for their identification, assessment, and regulatory management (Kortenkamp et al. 2011; WHO/IPCS 2002). In recent years, up to 800 substances have been listed as suspected endocrine disruptors by different organizations worldwide (EC/BKH 2000; WHO/UNEP 2013). Although a causal link between environmental contamination and the occurrence of adverse health effects is often difficult to establish, an excess of hormone-sensitive cancer types, particularly breast cancer, has for example been reported in a study of contaminated sites in Italy, where the presence of EDCs was documented (Benedetti et al. 2017). To ensure a high level of protection of human health, specific provisions on how to address EDCs according to scientific criteria were included in the EU legislations on pesticides, biocides and chemicals that strictly regulate the production and marketing of EDCs in the European Union (EC 2006; 2009; EU 2012).

Estrogens are essential hormones of the human endocrine system and exhibit a broad spectrum of physiological functions from development to reproduction and behavior (Fuentes and Silveyra 2019). Despite these beneficial functions, persistently elevated blood levels of estrogens are associated with an increased risk of breast cancer (Yager and Davidson

* Corresponding author at: German Federal Institute for Risk Assessment (BfR), German Centre for the Protection of Laboratory Animals (Bf3R), Max-Dohrn-Straße 8-10, 10589 Berlin, Germany.
E-mail address: Michael.Oelgeschlaeger@bfr.bund.de (M. Oelgeschläger).

https://doi.org/10.1016/j.envint.2021.106411
Received 13 November 2020; Received in revised form 11 January 2021; Accepted 18 January 2021
Available online 4 February 2021

2006), which is still the most frequent cancer type and leading cause of cancer deaths in women worldwide (Wild et al. 2020). The diverse pathological mechanisms leading to metastatic progression of epithelial-type tumors (carcinomas) such as breast cancer include the disruption of cell-cell contacts and tissue integrity due to the malignant destabilization of adherens junctions (AJs) (Berx and van Roy 2009). So far, this process is primarily been attributed to the partial or complete loss of the essential AJ protein E-Cadherin (E-Cad). However, E-Cad expression sustains in most metastasizing invasive ductal carcinomas (IDC), the most common type of breast cancer (Hashizume et al. 1996; Qureshi et al. 2006). We recently described a novel clinically-relevant mechanism, in which estrogens determine the spatial organization of AJs and the localization of E-Cad in human MCF-7 breast cancer cells through estrogen receptor (ER) alpha and the EGFR ligand amphiregulin Bischoff et al. (2020). We further found that these estrogen-dependent changes in cell-cell contact morphology influenced cell adhesion, cell stiffness, and cell motility, representing functional readouts that are often associated with breast cancer progression and metastatic potential (Bischoff et al. 2020).

Public concern regards the unintended exposure to industrial chemicals in the environment, food or consumer products that act as EDCs and influence estrogen levels or interfere with normal estrogen function, thereby leading to adverse health effects such as impaired reproduction and carcinogenesis (Giulivo et al. 2016; Johansson et al. 2017; La Merrill et al. 2020). In a regulatory context, the analysis of adverse health effects caused by environmental chemicals on endocrine-relevant endpoints including reproduction (OECD 2001; 2018a) and carcinogenicity (OECD 2018b;c;d) still requires complex *in vivo* assays that are approved under the OECD Test Guidelines (TG) Program. However, these *in vivo* assays are not specific for individual endocrine modes-of-action, are cost and time consuming, and require high numbers of test animals. Alternative test methods based on *in chemico* or *in vitro* approaches allow chemicals to be tested more specifically for estrogenic activity, but due to their design only capture single events of estrogen biogenesis (OECD 2011) or estrogen signaling, e.g. ER binding (OECD 2015) and transactivation (OECD 2016b). In order to meet the demand of reducing the number of animals that are globally used for the testing of environmental chemicals and to eventually fully replace traditional *in vivo* studies, there is an urgent need for equally reliable and functionally equivalent alternative test methods that address more complex human-relevant endpoints, including those that are associated with breast cancer progression and metastasis. To this end, multiple co-culture and three-dimensional (3D) cell culture models that, e.g., mimic the mammary tumor microenvironment or reconstitute the glandular organization of the breast tissue have emerged in recent years and facilitate the evaluation of potential endocrine effects of environmental chemicals on mammogenesis and breast tumor development (Caron-Beaudoin et al. 2017; Deng et al. 2020; Hudon Thibeault et al. 2014; Marchese and Silva 2012; Speroni et al., 2016; Speroni et al. 2014; Yancu et al. 2020).

However, considering the high and increasing number of industrial chemicals worldwide and the even more possible combinations thereof, novel test methods further need to be fit-for-purpose to be included into large-scale screening programs that facilitate the generation of concentration-response information to precisely measure the bioactivity of chemicals and mixtures for specific endpoints. In order to identify and prioritize chemicals with estrogenic properties, the U.S. EPA Toxicity Forecaster (ToxCast) project (Dix et al. 2007; Judson et al. 2010; Reif et al. 2010; Rotroff et al. 2013) integrates results from 18 automated high-throughput screening (HTS) assays into a computational model to derive an ER bioactivity score (Browne et al. 2015; Judson et al. 2015), which was validated against curated *in vivo* reference data from the uterotrophic bioassay in rodents (Kleinstreuer et al. 2016; OECD 2007). More recently, it was shown that a minimal set of four of the in total 18 ToxCast ER assays achieved a comparable performance to determine estrogen agonist activity (Judson et al. 2017). Although the ToxCast ER model combines single mechanistic events of estrogen signaling (ER binding, ER dimerization, regulation of gene expression, and proliferation) to derive an overall ER bioactivity score, the immediate relevance of the derived data with regard to the functional mechanisms that are involved in metastatic breast cancer progression and metastasis remains unclear.

Here, we describe the development of an image-based phenotypic screening assay, called E-Morph Assay, that is based on estrogen-dependent changes in the morphology of cell-cell contacts (Bischoff et al. 2020) as a novel functional and clinically-relevant endpoint to predict the estrogenic activity of environmental chemicals. The conceptual design of the E-Morph Assay bases on the competitive co-treatment of test substances with the anti-estrogen Fulvestrant, which is a widely used agent in second-line treatment of ER positive metastatic breast cancer. This way, the E-Morph Assay will provide new functional information that is complimentary to the mechanistic data from the existing OECD TG and ToxCast assays.

2. Materials and methods

2.1. Cell line and routine cell culture conditions

The MCF-7/vBOS (*Michigan Cancer Foundation-7/variantBOS*) cell line that is used in the E-Morph Assay was previously described and extensively characterized in Bischoff et al. (2020). It was particularly selected because of the high estrogen sensitivity of the parental MCF-7/BOS cell line (Soto and Sonnenschein, 1985), which was reported to respond to very low estrogen concentrations reaching a plateau already at 10 pM (Villalobos et al., 1995). The responsiveness of the MCF-7/vBOS cell line under anti-estrogenic and estrogenic conditions has been shown in Bischoff et al. (2020). The identity of MCF-7/vBOS cells as a derivative of the ATCC MCF-7 reference cell line (HTB-22) was verified by the ATCC STR profiling service (ATCC). MCF-7/vBOS cells were deposited for patent purposes under the accession number DSM ACC3321 at Leibniz Institute DSMZ-German Collection of Microorganisms and Cell Cultures. Routine cell cultures were maintained at 37 °C with 5% CO_2 in normal-serum medium (Dulbecco's modified Eagle's medium [DMEM, Biochrom], 10% (v/v) Fetal Bovine Serum [FBS, Biochrom, S0615, Estradiol levels: 18.6–22.3 pg/ml], 100 µg/ml streptomycin / 100 U/ml penicillin [Biochrom]). Cells were sub-cultured over a maximum of 8–10 passages, and regularly tested using the GATC mycoplasma test service (GATC Biotech).

2.2. E-Morph: Cell seeding, test substance exposure and assay plate layout

The E-Morph Assay was performed at 37 °C with 5% CO_2 in reduced-serum medium (phenol red-free DMEM [Gibco], 5% (v/v) FBS [Biochrom, S0615, Estradiol levels: 18.6–22.3 pg/ml], 2 mM stable glutamine, 100 µg/ml streptomycin / 100 U/ml penicillin [Biochrom]). The final Estradiol concentration in reduced-serum medium was in the range of 3.4–4.1 pM, which corresponds to physiological serum levels of postmenopausal women (Rothman et al. 2011). Cells were seeded into 96-well glass bottom ViewPlate microplates (PerkinElmer) at a concentration of 80,000 cells/well in 200 µl reduced-serum medium, grown until 80–90% confluency for 24 h, and then exposed to 200 µl reduced-serum medium containing test chemicals in combination with the anti-estrogen Fulvestrant (Fulv) for 48 h. The Fulv concentration in this exposure medium has been set to 10 nM, which was previously reported to be saturating with regard to the reorganization of the cell-cell contact morphology and the inhibition of estrogen-responsive gene expression (Bischoff et al. 2020). This Fulv concentration was further in the range of steady-state blood plasma levels (~20 nM) of patients undergoing anti-estrogen-based endocrine therapy (McCormack and Sapunar 2008).

Each test substance was, along with the solvent and Fulv controls, tested in 12 consecutive concentrations from 100 µM to 100 pM in technical triplicates allowing the simultaneous evaluation of two

different substances on a single 96-well plate (see assay plate layout in File S3). The lower boundary of 100 pM was selected based on the absence of detectable effects on cell-cell contact morphology when cells were exposed to very strong pharmaceutical estrogens, e.g. 17α-Ethinylestradiol and Diethylstilbestrol. The higher boundary of 100 μM was selected in order to ensure detection of very weak estrogenic activities of chemicals, to ensure a sufficient level of confidence in negative test results, and to verify exposure of cells by testing close to the limit of cytotoxicity. Notably, depending on the intended use (e.g. primary hit screening or precise potency determination) of the E-Morph Assay, other suitable concentration ranges may be identified, e.g., by performing range finding runs. Further adjustment of the 10 nM Fulv concentration would be a possible option to further fine-tune the assay. The following test substances were used: Fulvestrant (CAS-No. 129453-61-8), 17β-Estradiol (CAS-No. 50-28-2), Estrone (CAS-No. 53-16-7, Dihydrotestosterone (CAS-No. 521-18-6), Progesterone(CAS-No. 57-83-0), 17α-Ethinylestradiol (CAS-No. 57-63-6), Diethylstilbestrol (CAS-No. 56-53-1), Genistein (CAS-No. 446-72-0), Daidzein (CAS-No. 486-66-8), Coumestrol (CAS-No. 479-13-0), Bisphenol A (CAS-No. 80-05-7), Bisphenol B (CAS-No. 77-40-7), Bisphenol AF (CAS-No. 1478-61-1), Bisphenol S (CAS-No. 80-09-1), Ketoconazole (CAS-No. 65277-42-1), Atrazine (CAS-No. 1912-24-9), Reserpine (CAS-No. 50-55-5), Zearalenone (CAS-No. 17924-92-4). Ethanol and Dimethyl Sulfoxide (DMSO) were used as solvent control at a final concentration of 0.1% (v/v). All substances were purchased from Sigma-Aldrich. Exposure medium was exchanged on a daily basis.

2.3. E-Morph: Live-cell staining and high-content fluorescence microscopy

After treatment for 48 h, cells were stained in PBS containing 1 μM CellTrace Far Red (Molecular Probes) to visualize the cell-cell contact morphology and 20 μg/ml Hoechst 33342 to label nuclei (Molecular Probes) for 20 min at 37 °C with 5% CO_2, then washed twice with reduced-serum medium, and incubated for another 10 min at 37 °C with 5% CO_2 (see Fig. 1C). To test for cytotoxicity, cells were stained with 0.1X CellTox Green (Promega) in reduced-serum medium after the final washing step according to the manufacturer's protocol.

Immediately after staining, cells were imaged using a 40x water objective (NA 1.1) at 9 standardized positions per well and 10 optical sections with 2 μm spacing per position at an Opera Phenix high-content screening system (PerkinElmer), and subsequently analyzed using the integrated Harmony software or a CellProfiler/CellProfiler-Analyst-based image analysis pipeline as described below.

2.4. E-Morph: Quantitative image analysis

Quantitative image analysis was performed using customized image analysis pipelines that were built in the integrated Harmony software (Perkin Elmer) (see Fig. 1C-G′ and Figure S1A-E′) or using the CellProfiler (Carpenter et al. 2006) and CellProfiler Analyst (Jones et al. 2008) (CP/CPA) open-source software packages (see Figure S1F-H). Both image analysis pipelines generally comprise two main steps, *a)* the segmentation of cells and extraction of morphological parameters, and *b)* the subsequent parameter-based classification of cells by supervised machine learning. For each well, maximum intensity projections from acquired z-stacks of nine standardized positions were analyzed.

In the Harmony software-based image analysis pipeline, the segmentation of the nucleus (Hoechst 33342 channel) and cytoplasm (CellTrace channel) was performed using the *FindNuclei* module (method C) and the *FindCytoplasm* module (method A), respectively. Cells at the edges were excluded using the *SelectPopulation* module. Morphological parameters were extracted from the CellTrace channel using the *CalculateMorphologyProperties* module with activated STAR features. For parameter-based cell classification, supervised machine learning was conducted based on randomly selected cells from positive control (Fulv treatment) and negative control (solvent) wells using the *SelectPopulation* module (linear classifier method). This step defined the morphological parameters underlying the binary classification of cells that did not show any changes in cell-cell contact morphology ('negative' class, green) and cells displaying the Fulv-induced phenotype ('positive' class, magenta) (see Fig. 1D and Figure S1B). Training sets were assembled in a balanced way by selecting the same number of cells per class from each replicate experiment (see Fig. 1 and Figure S1: 60 cells per class and replicate [in total 180 cells]) or from each assay validation plate (see Figure S2: 40 cells per class and replicate [in total 360 cells]).

The final training set that was derived from the assay validation plates (see Figure S2) also served as the basis for the classification of all substance testing runs (see Figs. 3, 4 and Figure S3). During analysis of each individual run, this basic training set was complemented by additional selection of 50 cells per class from control wells of the respective screening plate (in total 410 cells) to compensate for plate-to-plate variations. The CellTox Green mean intensity (CellTox Green channel) was quantified using the *CalculateIntensity* module based on the before segmented nuclear regions.

As an open-source alternative to the commercial Harmony software, the CP/CPA-based image analysis pipeline was built in a very analogous way. Upon segmentation of nuclei (Hoechst 33342 channel, *PrimaryObjects* module, Otsu method), identification of the cytoplasm (CellTrace channel, *SecondaryObjects* module, watershed-gradient method), and exclusion of the cells at the edges of the image (border objects), morphological parameters were extracted using the *MeasureTexture* and *MeasureGranularity* modules, and exported from CP into a relational database along with a CPA properties file. For parameter-based cell classification, supervised machine learning was conducted in CPA in an analogous way as described above (*Classifier* module, random forest classifier method, 60 cells per class and replicate).

As with other fluorescence assays, the test chemicals may interfere with the fluorescence signal, e.g., by fluorescence quenching. In the E-Morph Assay, uniform influences on the fluorescence signal intensity are to a large extent not expected to be a major issue for the assay readouts, because the image analysis algorithm mainly depends on the relative distribution of pixel intensities. Therefore, uniform changes such as moderate increase of decrease of signal intensities that apply to the entire imaged region are unlikely to influence the results significantly. However, excessive depletion of the signal intensity would result in a poor signal-to-noise ratio and eventually more strongly affect the image analysis procedure. Such effects were not observed in this study, however, it might be considered to add an additional node into the image analysis procedure that reads out global signal intensities to control for such excessive interferences with the readout.

2.5. E-Morph: Morphology Index calculation

As described in Bischoff et al. (2020), the fraction of cells that did not show any changes in cell-cell contact morphology ('negative' class derived from quantitative image analysis) was represented as the Morphology Index (MI). First, the MI of each individual well was calculated:

$$\mathrm{MI}_{well} = \frac{\mathrm{Number\ of\ cells}^{NO\ \ change\ \ in\ \ cell-cell\ \ contact\ \ morphology}}{\mathrm{Number\ of\ cells}^{\ ALL\ \ cells}}$$

Second, the MI_{well} from technical replicates of the test substance concentrations and the solvent control (see plate layout in File S3) were each averaged:

$$\mathrm{MI}_{avr} = \frac{\mathrm{MI}_{well\_1} + \mathrm{MI}_{well\_2} + \mathrm{MI}_{well\_n}}{\mathrm{n}}$$

Third, the MI_{avr} of each test substance concentration (Substance) was normalized to the MI_{avr} of the corresponding solvent control (Solv) (see plate layout in File S3) to derive the final MI:

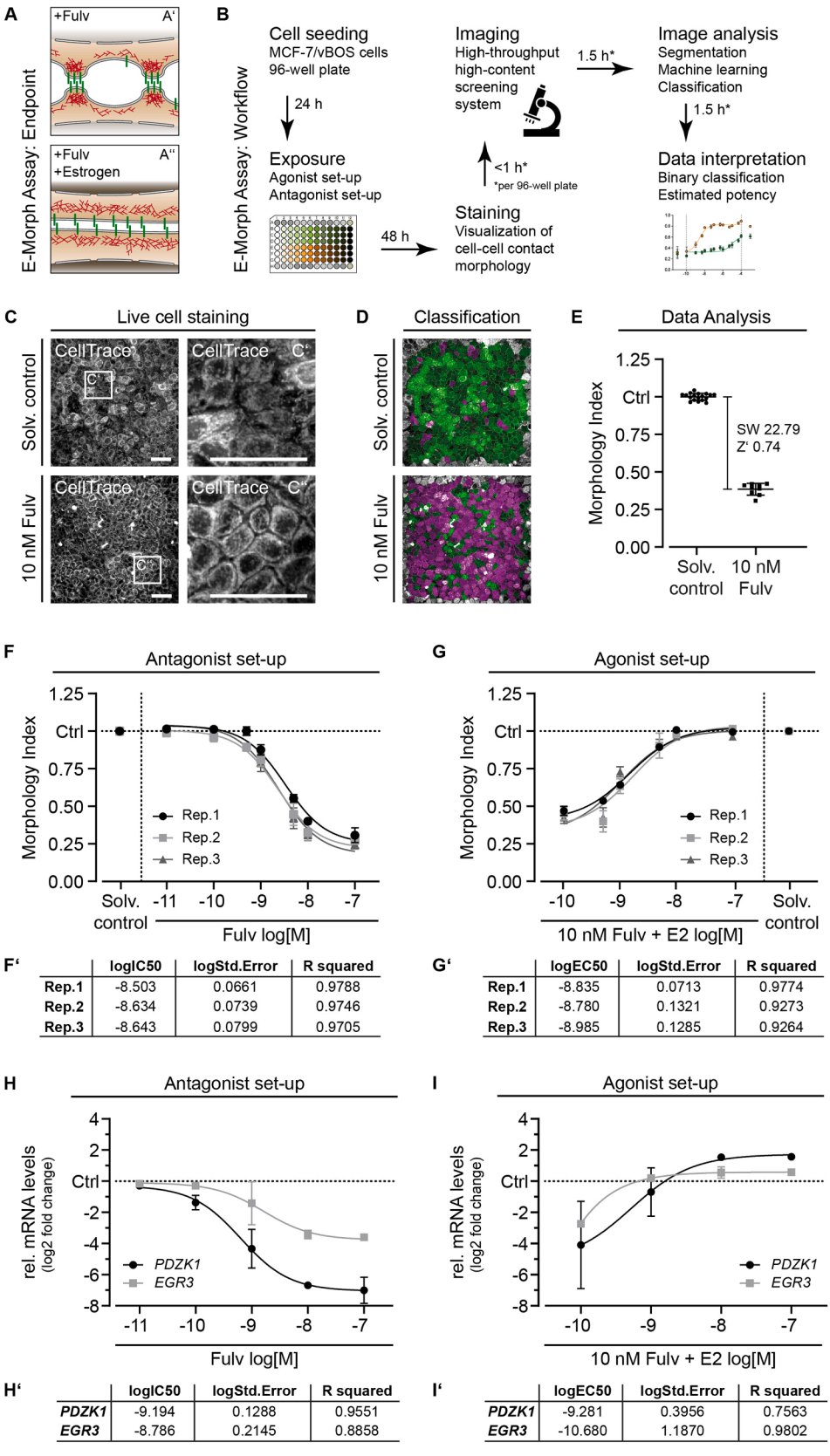

	logIC50	logStd.Error	R squared
Rep.1	-8.503	0.0661	0.9788
Rep.2	-8.634	0.0739	0.9746
Rep.3	-8.643	0.0799	0.9705

	logEC50	logStd.Error	R squared
Rep.1	-8.835	0.0713	0.9774
Rep.2	-8.780	0.1321	0.9273
Rep.3	-8.985	0.1285	0.9264

	logIC50	logStd.Error	R squared
PDZK1	-9.194	0.1288	0.9551
EGR3	-8.786	0.2145	0.8858

	logEC50	logStd.Error	R squared
PDZK1	-9.281	0.3956	0.7563
EGR3	-10.680	1.1870	0.9802

Fig. 1. Visualization and quantification of cell-cell contact morphology as an endpoint for estrogenic activity in the E-Morph Assay. (A) Graphical representation of the phenotypic readout that is used as an endpoint in the E-Morph Assay to measure the estrogenic potential of substances. Treatment of MCF-7 breast cancer cells with the anti-estrogen Fulvestrant (Fulv) leads to a reorganization of adherens junctions (AJ) and an increased spacing between adjacent cells (A′), which can be prevented by co-treatment with estrogens (A″). The cell-cell adhesion protein E-Cadherin is depicted in green and the cortical actomyosin cytoskeleton in red. (B) Workflow of the E-Morph Assay showing key steps and their duration from cell seeding to the final classification of a test substance. (C) Fluorescence images showing intercellular spacing upon Fulv treatment for 48 h as compared to the solvent control. White boxes indicate enlarged cell membrane areas shown in C′-C″. Scale bars, 25 μM. (D) Color-coded representation of classifications obtained from quantitative image analysis of CellTrace-stained cells using the Harmony software. Cells showing the Fulv-induced phenotype are highlighted in magenta. Cells showing no detectable changes in cell-cell contact morphology are indicated in green. (E) Representative results from Harmony software-based quantitative image analysis of CellTrace-stained cells treated with Fulv for 48 h and solvent control-treated cells. The plot depicts the Morphology Index (MI), which represents the fraction of cells that do not show any detectable changes in cell-cell contact morphology (green) normalized to the solvent control (Ctrl). The reorganization of AJs upon Fulv treatment results in a decrease of the MI. Each data point shows the MI from a single well. Nine images were recorded per well. The signal window (SW) and Z′-factor (Z′) indicate the separation of the measured MI values (effect size) between positive control (Fulv treatment) and negative control (solvent) wells according to Iversen et al. (2012). Biological replicates, n = 3. Error bars, mean ± SD. (F,G) Application of the Harmony software-based image analysis pipeline to measure the MI of CellTrace-stained cells that were treated with (F) increasing concentrations of Fulv (antagonist set-up) or (G) increasing concentrations of 17β-estradiol (E2) in the presence of 10 nM Fulv (agonist set-up) for 48 h. Each data point represents an average MI from three wells per treatment condition and nine images per well (in total 27 images). Error bars, mean ± SD of three technical replicates. Biological replicates, n = 3. (F′,G′) Half-maximal concentrations derived from dose-response curves shown in (F,G). Non-linear fit (three parameters, hill slope = 1). (H,I) Quantitative PCR measurement of mRNA expression levels of typical ERα target genes (*PDZK1*; *EGR3*) of cells treated as shown in (F,G). Relative mRNA expression levels for each treatment condition are normalized to the solvent control (Ctrl). Biological replicates, n = 3. Error bars, mean ± SD. (H′,I′) Half-maximal concentrations derived from dose-response curves shown in (H,I). Non-linear fit (three parameters, hill slope = 1). (For interpretation of the references to color in this figure legend, the reader is referred to the web version of this article.)

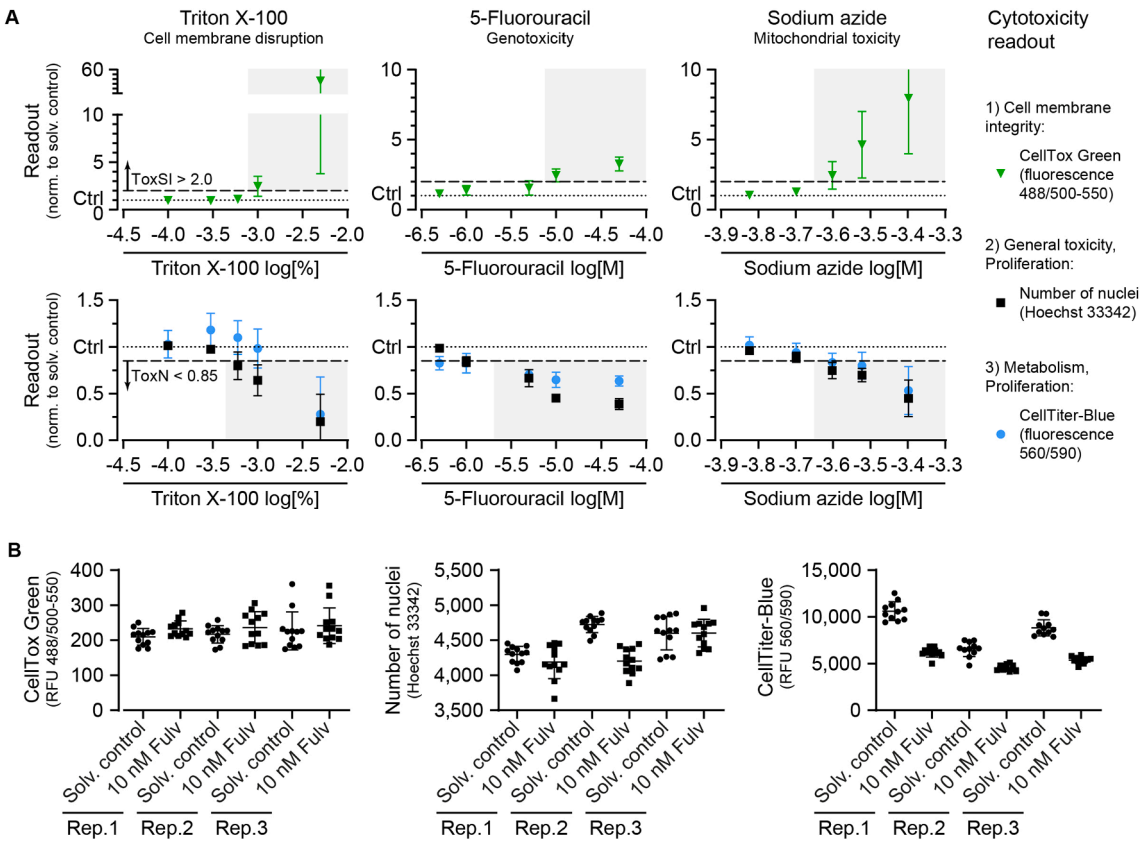

Fig. 2. Evaluation of fluorescence microscopy-based cytotoxicity readouts of the E-Morph Assay. A) Detection of cytotoxic effects upon treatment of cells for 48 h with increasing concentrations of Triton X-100, 5-Fluorouracil, and Sodium azide using CellTox Green intensity, Number of nuclei derived from Hoechst 33342 staining, and CellTiter-Blue intensity as readouts. The readout of each treatment condition is normalized to the solvent control (Ctrl). Each data point represents an average signal readout from three wells per treatment condition and nine images per well (in total 27 images) of three biological replicates. Error bars, mean ± SD. The dashed lines show defined thresholds indicating excessive cytotoxicity of specific concentration ranges (grey zones). ToxSI, toxicity threshold based on the CellTox Green nuclear signal induction. ToxN, toxicity threshold based on the number of nuclei. B) Influence of Fulv treatment for 48 h on the indicated cytotoxicity readouts as compared to the solvent control. Each data point represents an average signal readout from nine images per well. Biological replicates, n = 3. Error bars, mean ± SD. (For interpretation of the references to color in this figure legend, the reader is referred to the web version of this article.)

$$\mathrm{MI} = \frac{\mathrm{MI}_{avr}^{Substance}}{\mathrm{MI}_{avr}^{Solv}}$$

2.6. E-Morph: Quality assessment and cytotoxicity determination

For quality assessment, the signal separation (effect size) was determined for each run using the two commonly used statistical parameters signal window (SW) and Z′-factor (Z′) according to Iversen et al. (2012). The SW and Z′ was calculated based on the average MI (MI_{avr}) and the standard deviation (MI_{sd}) of the positive control (Fulv) and negative control (Solv) wells that correspond to each test substance (see plate layout in File S3):

$$\mathrm{SW} = \frac{\left(\mathrm{MI}_{avr}^{Solv} - 3\mathrm{MI}_{sd}^{Solv}/\sqrt{3}\right) - \left(\mathrm{MI}_{avr}^{Fulv} + 3\mathrm{MI}_{sd}^{Fulv}/\sqrt{3}\right)}{\mathrm{MI}_{sd}^{Solv}/\sqrt{3}}$$

$$\mathrm{Z}^{`} = \frac{\left(\mathrm{MI}_{avr}^{Solvent} - 3\mathrm{MI}_{sd}^{Solvent}/\sqrt{3}\right) - \left(\mathrm{MI}_{avr}^{Fulv} + 3\mathrm{MI}_{sd}^{Fulv}/\sqrt{3}\right)}{\mathrm{MI}_{avr}^{Solvent} - \mathrm{MI}_{avr}^{Fulv}}$$

The acceptance criterion for a valid run was SW > 2 or Z′ > 0.4 (see Fig. 4).

Cytotoxicity of each test substance concentration (Substance) was determined based on the average number (N) of Hoechst 33342 stained nuclei (ToxN) and the average nuclear signal induction (SI) of the CellTox Green dye (ToxSI) from technical replicate wells relative to the corresponding Fulv control (Fulv) (see plate layout in File S3):

$$\mathrm{ToxN} = \frac{\mathrm{N}_{avr}^{Substance}}{\mathrm{N}_{avr}^{Fulv}}$$

$$\mathrm{ToxSI} = \frac{\mathrm{SI}_{avr}^{Substance}}{\mathrm{SI}_{avr}^{Fulv}}$$

Excessive cytotoxicity of a test substance concentration was indicated by ToxN < 0.85 or ToxSI > 2.0 and led to the exclusion of the corresponding wells from further analysis (see Fig. 4).

2.7. E-Morph: Test substance classification and potency estimation

The overall binary classification (POS or NEG) of a test substance (see Fig. 4) was derived by applying a '2-out-of-3' approach based on the maximal MI (MI_{max}) that was obtained from three independent runs (biological triplicates). A test substance was classified as overall positive (POS) or negative (NEG) when the MI_{max} was above (Pos) or below (Neg) the threshold MI of 0.75 in at least two independent runs, respectively.

The potency of a test substance was estimated based on the interpolated concentration (MI75) at which an MI of 0.75 (threshold indicating estrogenic activity) was reached. The MI75 concentration was calculated for each test run by linear interpolation of the two adjacent tested concentrations (conc) that resulted in an MI right below (b) and right above (a) the threshold MI of 0.75 using the following equation:

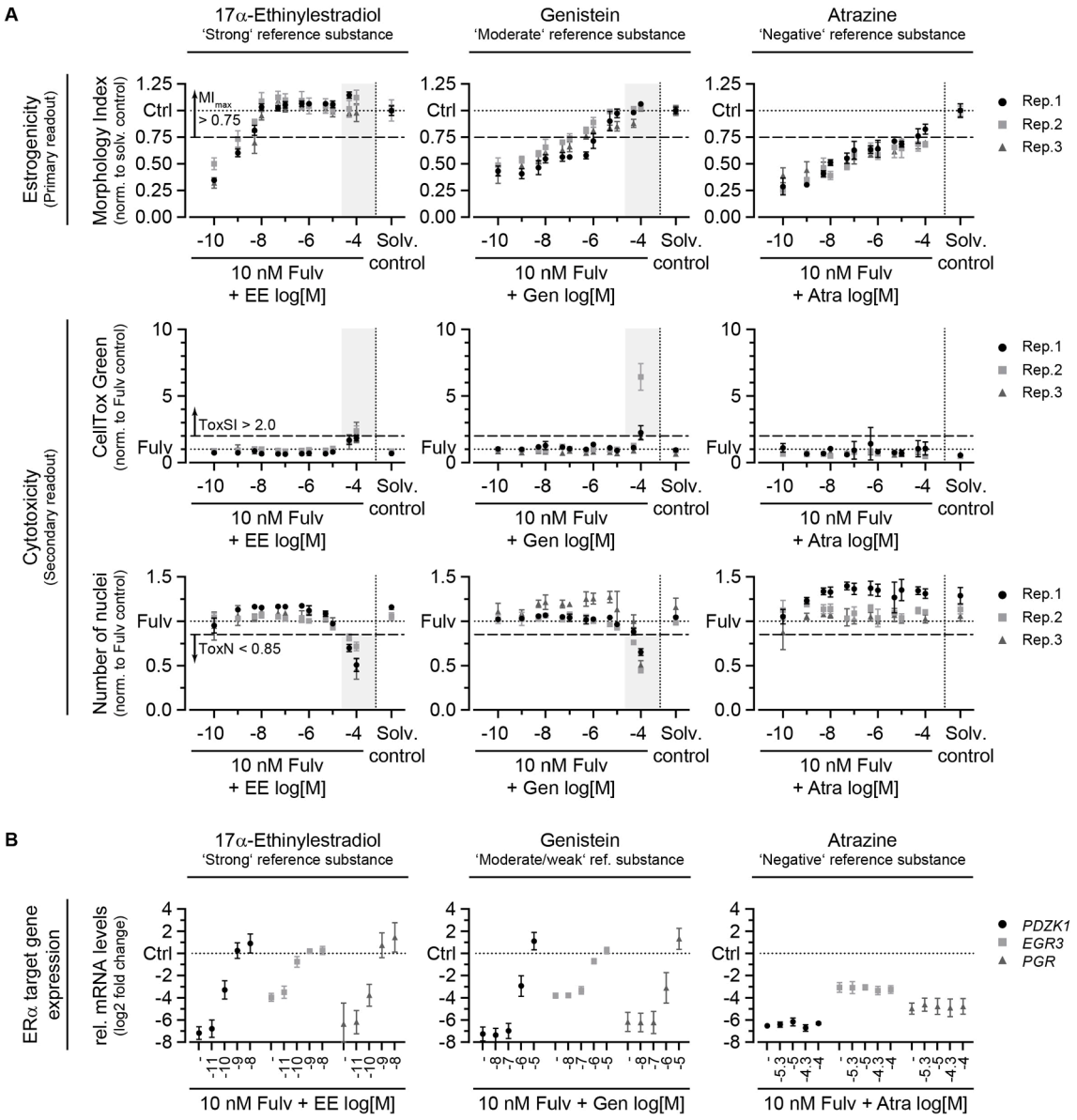

Fig. 3. Definition of a threshold for separation of estrogenic from non-estrogenic substances in the E-Morph Assay. A) MI of cells treated with increasing concentrations of the indicated reference substances. The dashed lines show defined thresholds indicating estrogenic effects (MI_{max}) or cytotoxic effects (ToxSI; ToxN) of a test substance. The grey zones indicate concentration ranges for which excessive cytotoxicity was detected (ToxN < 0.85 or ToxSI > 2.0). Each data point represents an average MI from three wells per treatment condition and nine images per well (in total 27 images). Error bars, mean ± SD of three technical replicates. Biological replicates, n = 3. B) Quantitative RT-PCR measurement of mRNA expression levels of typical ERα target genes (*PDZK1*; *PGR*; *EGR3*) of cells treated as shown in (A). Relative mRNA expression levels for each treatment condition are normalized to the solvent control (Ctrl). Biological replicates, n = 3. Error bars, mean ± SD.

$$\mathrm{MI75} = conc_b + \frac{(0.75 - MI_b)^*(conc_a - conc_b)}{(MI_a - MI_b)}$$

If applicable, EC50 concentrations were directly derived from MI dose-response curves of test substances with sufficiently strong estrogenic activity, i.e. substances whose MI values fully reached the level of the solvent control (MI = 1.00).

The estimated potencies (MI75 or EC50) for each tested substance (Substance) were further converted into a relative ER bioactivity score by normalization of the median logMI75 or median logEC50 values (derived from three independent runs) to the median of the potent estrogen 17α-Ethinylestradiol (EE):

$$\mathrm{ER\ \ Bioactivity} = \frac{\mathrm{Median}(\mathrm{LogMI75}_{run\_1}; \mathrm{LogMI75}_{run\_2}; \mathrm{LogMI75}_{run\_n})^{Substance}}{\mathrm{Median}(\mathrm{LogMI75}_{run\_1}; \mathrm{LogMI75}_{run\_2}; \mathrm{LogMI75}_{run\_n})^{EE}}$$

The same approach was undertaken in this study to normalize available potency data from established *in vivo* [OECD TG 440] and *in vitro* [OECD TG 493, 455] test methods (OECD 2007; 2015; 2016b). In the U.S. EPA ToxCast project, EE was also used as a reference to derive the ToxCast ER model score (Browne et al. 2015; Judson et al. 2015). Hence, this conversion of potency data facilitates the activity-based grouping of the tested substances and a direct comparison of the test results from the E-Morph Assay to existing ER assays.

2.8. Quantitative PCR

RNA extraction (RNeasy Kit, Qiagen), cDNA synthesis (High-Capacity cDNA Reverse Transcription Kit, Applied Biosystems), and quantitative PCR (qPCR) (PowerUp SYBR Green Master Mix, ThermoFisher) were conducted as described in Bischoff et al. (2020) using a QuantStudio 7 Flex Real-Time PCR System (Applied Biosystems) (40

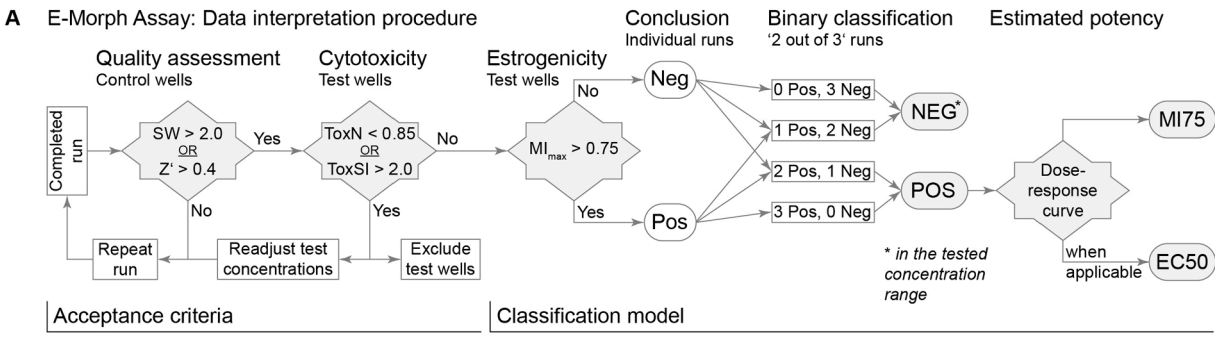

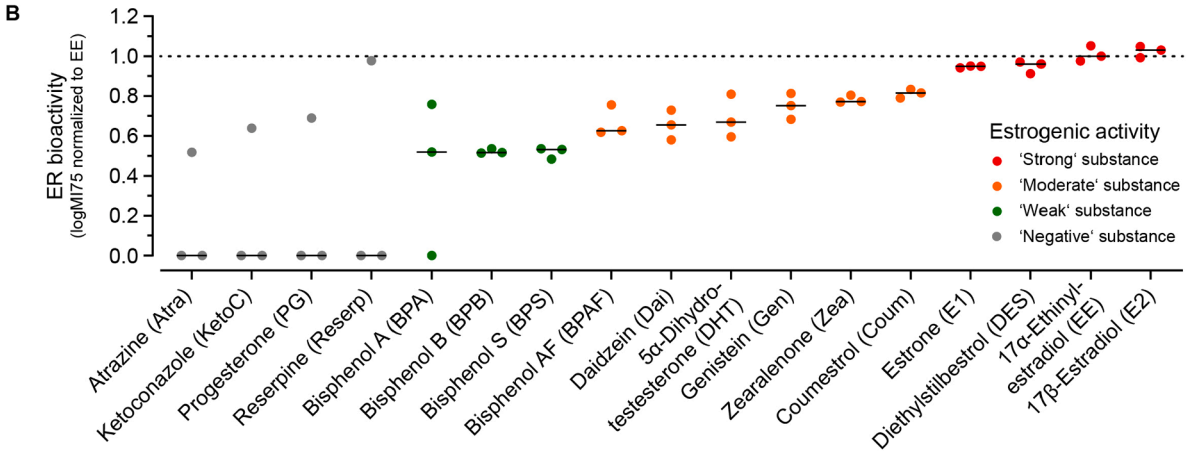

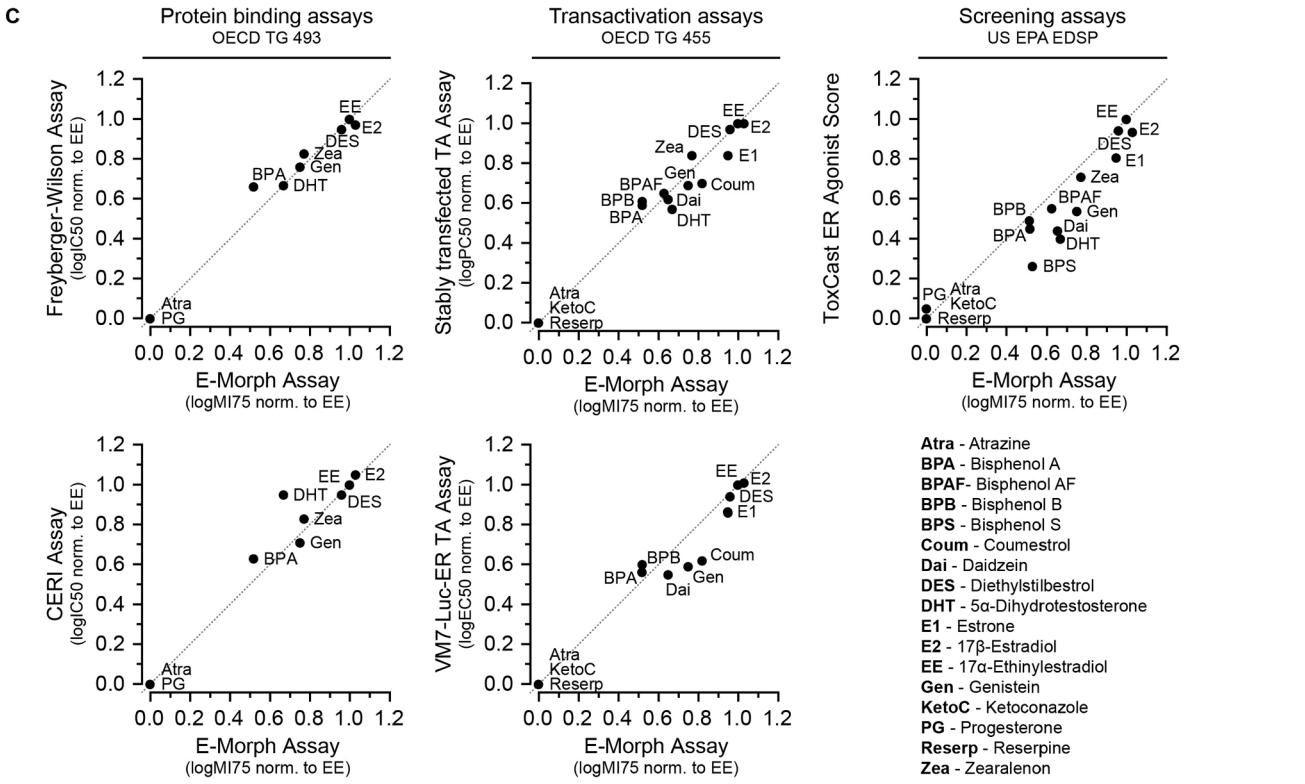

(caption on next page)

Fig. 4. Evaluation of the classification model and predictive capacity of the E-Morph Assay. A) Flow chart describing the data interpretation procedure that includes acceptance criteria for a valid run and a classification model to identify and characterize estrogenic substances. See main text for detailed description. SW, Signal window; Z′, Z′-factor; ToxSI, toxicity threshold based on the CellTox Green nuclear signal induction relative to the Fulv control; ToxN, toxicity threshold based on the number of nuclei relative to the Fulv control; MI_{max}, highest MI value measured for each substance at any non-cytotoxic test concentration; MI75, interpolated concentration at which the MI equals 0.75. B) Relative ER bioactivity of 17 tested substances. The estimated potencies (logMI75) of each individual substance are normalized to the median logMI75 of the potent estrogen 17α-Ethinylestradiol (EE). The substances are ranked and color-coded according to their relative estrogenic activity. Each data point represents the relative bioactivity (logMI75) obtained from three individual runs. The black line indicates the median of the indicated data points. Biological replicates, n = 3. C) Correlation between the relative ER bioactivities obtained from the E-Morph Assay and published *in vivo* and *in vitro* reference data as well as screening data from the ToxCast project. Each data point represents the median of the relative bioactivities obtained from three individual runs shown in (B). The contour line indicates full correlation. (For interpretation of the references to color in this figure legend, the reader is referred to the web version of this article.)

cycles; denaturation for 15 s at 95 °C; annealing, extension, and fluorescence read for 1 min at 60 °C). RNA expression levels (fold change) were calculated according to the $\Delta\Delta C_T$ method. Tyrosine 3-Monooxygenase/Tryptophan 5-Monooxygenase Activation Protein, Zeta (YWHAZ) served as housekeeping gene. Primers used (5′-3′ orientation):

EGR3 (GGTGACCATGAGCAGTTTGC, ACCGATGTCCATTACATTCTC TGT);

PDZK1 (CTCCAGCTCCTACTCCCACT, ACCGCCCTTCTGTACCTCTT);

PGR (TCAACTACCTGAGGCCGGAT, GCTCCCACAGGTAAGGACAC);

YWHAZ (ACTTTTGGTACATTGTGGCTTCAA, CCGCCAGGACAAACC AGTAT).

2.9. Immunofluorescence microscopy

Cells for immunofluorescence staining (see Figure S1A) were grown and treated according to the E-Morph Assay protocol described above. Staining was performed following the protocol described in Bischoff et al. (2020). Antibodies/dyes used: anti-E-Cadherin (H-108, Santa Cruz, 1:100); secondary antibody conjugated to Alexa Fluor 488 (Invitrogen, 1:100); DAPI (Roche). All images were acquired using an Opera Phenix high-content screening system (Perkin Elmer) and analyzed using the integrated Harmony software as described above.

2.10. Evaluation of cytotoxicity readouts and CellTiter-Blue cell viability assay

For evaluation of the phenotypic screening-compatible cytotoxicity read-outs (CellTox green nuclear intensity and number of nuclei), cells were grown, treated, imaged, and analyzed according to the E-Morph Assay protocol described above. The following cytotoxic substances were used: Sodium azide (CAS-No. 26628-22-8), 5-Fluorouracil (CAS-Nr.51-21-8), and Triton X-100 (CAS-No. 9002-93-1) (all Sigma-Aldrich). The CellTiter-Blue cell viability assay (Promega) was performed immediately after high-content imaging of the 96-well plate. Cells were incubated in 200 μl of fresh reduced-serum medium containing 20 μl of the CellTiter-Blue reagent for 2 h at 37 °C with 5% CO_2. After incubation, 100 μl of the medium were transferred into black 96-well microtiter plates (Brand) and the fluorescence intensity was measured at 560_{Ex}/590_{Em} using a microplate reader (Tecan).

2.11. Statistical analysis and data visualization

Calculations were performed in Microsoft Excel 2016. Statistical analyses and graphical visualizations of data were performed using the GraphPad Prism 8 software. Dose-response curves were fitted using the non-linear fit algorithm (three parameters, hill slope = 1) to derive half-maximal concentrations (IC50, EC50). Figures were generated using Adobe Illustrator CC 2020.

3. Results and discussion

3.1. Visualization and quantification of substance-specific effects on cell-cell contact morphology

The conceptual design of the E-Morph Assay is based on our previous findings *a)* that treatment of MCF-7 breast cancer cells with the anti-estrogen Fulvestrant (Fulv) led to a striking reorganization of the cell-cell contact morphology at the level of adherens junctions (AJs) with an increased, bubble wrap-like spacing between adjacent cells (Fig. 1A′), and *b)* that this effect could be prevented by co-treatment with the potent, endogenous estrogen 17β-Estradiol (E2) (Fig. 1A″) in a dose-dependent manner (Bischoff et al. 2020). In addition, we have shown that this AJ reorganization correlated with an increase of cell stiffness and cell-cell adhesion but a decrease in cell motility, representing key parameters of metastatic cancer progression (Bischoff et al. 2020). We therefore reasoned that this estrogen-dependent change in cell-cell contact morphology could serve as a novel functional and clinically-relevant endpoint for the identification and characterization of estrogenic substances by image-based high-throughput screening (HTS).

The workflow of the E-Morph Assay is shown in Fig. 1B. In sum, the MCF-7/vBOS cells are grown for 24 h until 80–90% confluency is ensured and subsequently exposed for 48 h to 10 nM Fulv in combination with increasing concentrations of the test substances in a 96-well plate format (see materials and methods). Application of a cytoplasmic live cell dye, e.g. CellTrace, allows visualization of the characteristic increased spacing between adjacent cells upon Fulv treatment and avoids the need of performing labor-intensive immunofluorescence staining of AJ components (Fig. 1C; Figure S1A). An automated imaging and quantitative image analysis pipeline that deploys a high-content screening system, e.g. Opera Phenix, and integrated image analysis software, e.g. Harmony, facilitates efficient generation of dose-response data for multiple test substances within only a few hours.

The image analysis procedure includes two main steps, i.e. *a)* the automatic detection of cell outlines (segmentation) and extraction of morphological parameters, and *b)* a supervised machine learning approach to classify each individual cell based on its cell-cell contact morphology (classification) (see materials and methods). After supervised training of the classification algorithm using selected cells from solvent (negative) control and Fulv-treated (positive) control wells, the image analysis software automatically identifies cells that do not show any changes in cell-cell contact morphology (Fig. 1D and Figure S1B, green) and cells displaying the Fulv-induced phenotype (Fig. 1D and Figure S1B, magenta). Importantly, a sufficiently trained classification algorithm can be applied to analyze multiple well plates and, if required, be further fine-tuned to compensate for plate-to-plate variations across multiple runs. Finally, the fraction of cells that do not show any changes in cell-cell contact morphology is represented as the Morphology Index

(MI) as described in Bischoff et al. (2020) (Fig. 1E; Figure S1C) (see materials and methods). Under estrogenic conditions, the MI is in the range of the solvent control (MI = 1.00) and reduced by selective ER inhibitors, like Fulv (Fig. 1E; Figure S1C).

To verify the ability of the E-Morph Assay to reliably detect estrogen-dependent changes in cell-cell contact morphology, we determined the MI upon treatment with increasing concentrations of Fulv alone (antagonist set-up), or with a fixed concentration of 10 nM Fulv in combination with increasing concentrations of E2 (agonist set-up) using CellTrace live cell staining (Fig. 1F-G′) and E-Cad immunofluorescence staining (Figure S1D-E′). Clear dose-dependent changes of the MI were detected for both set-ups and for both staining methods, which further correlated well with changes in mRNA expression levels of the estrogen receptor alpha (ER) target genes *PDZK1* and *EGR3* (Fig. 1H-I′). The effective IC50 and EC50 concentrations of Fulv and E2 (in presence of 10 nM Fulv) were in the range of 1–10 nM, which correlated very well with the published relative ERα-binding affinities of the two compounds in a competitive situation (Wakeling et al. 1991). This data supports the use of the MI as a reliable primary assay readout to determine estrogenic and anti-estrogenic activity in a phenotypic screening approach.

To demonstrate the cross-platform interoperability of the E-Morph Assay, we built an analogous image analysis pipeline using the user-friendly open-source CellProfiler/CellProfiler Analyst (CP/CPA) software (see materials and methods), and reanalyzed the high-content image data shown in Fig. 1F-G′. The resulting logIC50 (antagonist set-up) and logEC50 (agonist set-up) values as well as the variability of the measurements were highly concordant between the two image analysis pipelines (Fig. 1F-G′ and Figure S1F-H). These data verify that the obtained results were independent of the screening platform and image analysis software used and indicate that the E-Morph Assay can be readily integrated into diverse commercial and non-commercial screening platforms.

3.2. Evaluation of the Morphology Index as a primary assay readout for phenotypic screening

The applicability of the MI as a primary assay readout to robustly detect estrogenic substances was further evaluated with regard to two essential criteria describing the robustness of phenotypic screening assays, i.e. the signal separation (effect size) and the spatial uniformity of measurements (plate drift) (Iversen et al. 2012). This evaluation was performed by running the E-Morph Assay on three plates per day (intra-day variability) at three independent days (inter-day variability) (Figure S2A-B′), and the results were analyzed using a data evaluation template published by (Iversen et al. 2012) (File S1). The signal separation between the negative and positive controls including the deviation of values within each control group was evaluated using two commonly used statistical parameters, i.e. the signal window (SW) and Z′-factor (Z′) (see materials and methods). For the 48 h exposure time point, each run passed the recommended signal separation acceptance criteria in terms of SW $>$ 2.0 or Z′ $>$ 0.4 (Figure S2A-A′; File S1) demonstrating the robustness of the E-Morph Assay. In addition, no predominant patterns of plate drift or edge effects that would significantly affect the primary assay readout were observed in the spatial uniformity analysis (File S1). The effect size of the assay however declined when the test chemical exposure time was reduced to 30 h (Figure S2B-B′; File S2) indicating that the 48 h time point reported before (Bischoff et al. 2020) was also optimal for screening purposes. Together, the estrogen-dependency of the endpoint and the robustness of the primary assay readout provide a sound basis for the application of the E-Morph Assay in an image-based phenotypic screening approach to identify and characterize substances with estrogenic activity.

3.3. Implementation of additional secondary assay readouts detecting cytotoxicity

To control for potential side effects of test substances that may influence the primary assay readout, the E-Morph Assay was further complemented with two additional phenotypic screening-compatible endpoints, i.e. cell membrane integrity and number of cells, that allow determination of cell viability and detection of cytotoxicity (Fig. 2A-B). The non-membrane permeable CellTox Green dye, which only emits fluorescence signals upon intercalation into DNA of membrane-damaged cells, can be used as an indicator for perturbations of cellular function, e.g. cell membrane integrity, leading to reduced cell viability and eventually cell death (Riss et al. 2004). Furthermore, influences of test substances on the number of cells, e.g. due to excessive cell death or altered cell proliferation, can be readily identified by counting the number of nuclei after staining with a nuclear dye, e.g. Hoechst 33342. The applicability of the two additional secondary assay readouts, i.e. CellTox Green nuclear intensity and number of nuclei, was evaluated by treating cells for 48 h with increasing concentrations of the three known cytotoxic substances Triton X-100, 5-Fluorouracil, and Sodium azide that perturb cellular function through different modes-of-action (Fig. 2A). As expected, the CellTox Green nuclear intensity increased in a dose-dependent manner (Fig. 2A, green), while the number of cells decreased (Fig. 2A, black). Comparing these results with the commonly used but phenotypic screening-incompatible fluorometric CellTiter-Blue cell viability assay (Fig. 2A, blue), which measures the metabolic capacity of cells, confirms that CellTox Green nuclear intensity and the number of cells are reliable readouts to detected cytotoxic effects.

Based on these dose-response curves, appropriate thresholds indicating cytotoxicity of a test chemical in the E-Morph Assay were defined for the CellTox Green nuclear intensity (nuclear signal induction relative to the Fulv control, ToxSI $>$ 2.0) and the number of cells (number of nuclei relative to the Fulv control, ToxN $<$ 0.85) readouts (Fig. 2, dashed lines and grey zones) (see materials and methods). The threshold for ToxSI, 2.0, was applied to detect a significant and robust increase of the CellTox Green nuclear intensity relative to the control. The threshold for ToxN, 0.85, was selected to be in the range of the commonly used 20% cut-off indicating cytotoxicity in other ER *in vitro* assays (OECD 2016b). Both thresholds indicate cytotoxicity at very comparable concentration ranges and were used in the E-Morph Assay to identify maximal relevant testing concentrations and to exclude individual test wells from further analysis that show excessive cell death.

Since cells in the E-Morph Assay are treated with test substances in combination with a fixed concentration of Fulv, we also evaluated whether Fulv treatment on its own influenced these cytotoxicity readouts (Fig. 2B). When compared to the solvent control, Fulv only slightly influenced the average CellTox Green nuclear intensity (1.07 to 1.11-fold) and the number of cells (0.89 to 1.00-fold) within each replicate experiment, which was well below the ToxSI and ToxN thresholds. However, the CellTiter-Blue readout was more strongly affected by Fulv treatment (0.58 to 0.69-fold), which is in line with a previously described disruptive effect of Fulv on cellular metabolism (Warth et al. 2019). Together, these data support the use of CellTox Green nuclear intensity and the number of nuclei as suitable readouts to detect cytotoxicity in the E-Morph Assay.

3.4. Acceptance criteria and classification model

In order to identify and characterize environmental chemicals with estrogenic activity in the E-Morph Assay, we introduced an appropriate threshold that allowed separation of estrogenic from non-estrogenic

Table 1
Reference substances tested in the E-Morph Assay.

Chemical name	CAS No.	MeSH Chemicals class[a)]	MeSH Chemical action[b)]	Sources	E-Morph Assay reference chemical
17β-Estradiol	50-28-2	Polycyclic compounds > Steroids	Estrogens	Natural hormone; Pharmaceutical > Antimenopausal agent	Proof-of-concept study
17α-Ethinylestradiol	57-63-6	Polycyclic compounds > Steroids	Estrogens	Synthetic estrogen; Pharmaceutical > Contraceptive agents	Assay development
Diethylstilbestrol	56-53-1	Hydrocarbons, cyclic > Stilbenes	Estrogens, non-steroidal	Synthetic estrogen; Pharmaceutical > Rarely used due to ist cancerogenic effect	Assay development
Estrone	53-16-7	Polycyclic compounds > Steroids	Estrogens	Natural hormone; Pharmaceutical > Antimenopausal agent	Proof-of-concept study
Coumestrol	479-13-0	Heterocyclic compounds > Flavonoids	Estrogens, non-steroidal; Phytoestrogens	Natural product (Daidzein derivative)	Proof-of-concept study
Zearalenone	17924-92-4	Hydrocarbons, cyclic > Phenols > Resorcinols	Estrogens, non-steroidal	Natural product > Mycotoxins	Proof-of-concept study
Genistein	446-72-0	Heterocyclic compounds > Flavonoids	Estrogens, non-steroidal; Phytoestrogens; Protein kinase inhibitors	Natural product; Pharmaceutical > Anticarcinogenic agents	Assay development
5α-Dihydrotestesterone	521-18-6	Polycyclic compounds > Steroids	Androgens	Natural hormone	Proof-of-concept study
Daidzein	486-66-8	Heterocyclic compounds > Flavonoids	Estrogens, non-steroidal; Phytoestrogens	Natural product	Proof-of-concept study
Bisphenol AF	1478-61-1	Hydrocarbons, cyclic > Phenols	Endocrine disruptors	Industrial chemical > Manufacturing (plastics, rubber products)	Proof-of-concept study
Bisphenol S	80-09-1	Hydrocarbons, cyclic > Phenols	NA	Industrial chemical > Manufacturing (plastics) > Food contact material > Consumer products	Proof-of-concept study
Bisphenol B	77-40-7	Hydrocarbons, cyclic > Phenols	NA	Industrial chemical > Food contact material	Proof-of-concept study
Bisphenol A	80-05-7	Hydrocarbons, cyclic > Phenols	Estrogens, non-steroidal	Industrial chemical > Manufacturing (plastics, epoxy resins, …) > Food contact material > Consumer products	Assay development
Reserpine	50-55-5	Heterocyclic compounds > Indole alkaloids	Adrenergic uptake inhibitors; Adrenergic antagonists	Pharmaceutical > Antidepressant agents > Antipsychotic agents > Antihypertensive agents	Assay development
Progesterone	57-83-0	Polycyclic compounds > Steroids	Progestins	Natural hormone; Pharmaceutical > Contraceptive agents	Proof-of-concept study
Ketoconazole	65277-42-1	Heterocyclic compounds > Piperazines	14-alpha demethylase inhibitors; Cytochrome P-450 CYP3A inhibitors	Pharmaceutical > Antifungal agents	Proof-of-concept study
Atrazine	1912-24-9	Heterocyclic compounds > Triazines	Photosynthesis inhibitors	Agrochemical > Herbicide	Assay development

A total of 17 reference substances with known estrogenic properties were used to develop the E-Morph Assay and to evaluate its predictive capacity. Substances were assigned into chemical classes and modes-of-action using the U.S. National Library of Medicine's Medical Subject Headings (MeSH) categorization system. NA, no information available.

[a)] PubChem Classification Browser, MeSH node 'Chemicals and Drugs Category'.

[b)] PubChem Classification Browser, MeSH node 'Chemical Actions and Uses'.

substances based on the highest measured MI value for each substance (maximal MI, $MI_{max} > 0.75$) at any non-cytotoxic test concentration. This threshold has been defined using a set of six reference substances (OECD 2012) with known estrogenic activity (Table 1; Fig. 3A; Figure S3A). The two 'strong' reference substances 17α-Ethinylestradiol (EE) and Diethylstilbestrol (DES) showed a clear dose-dependent increase of the MI, which fully reached the level of the solvent control (MI = 1.00) at multiple test concentrations starting from 10 nM (EE) and 100 nM (DES), respectively. The MI of the 'moderate' reference substance Genistein (Gen) reached the level of the solvent control only at the highest non-cytotoxic concentration in the μM-range. Although the MI of the 'weak' reference substance Bisphenol A (BPA) increased in a dose-dependent manner, it did not reach the level of the solvent control at any non-cytotoxic concentration indicating that it could not fully compensate for the Fulv-induced effect. Albeit the MI of the 'negative' reference substances Atrazine (Atra) and Reserpine (Reserp) slightly increased as well, it rarely reached an MI value beyond 0.75 at non-cytotoxic concentrations. According to these results, an MI value of 0.75 was defined as a suitable cut-off that allows separation of estrogenic from negative reference substances. The relevance of the 0.75 threshold was further confirmed by monitoring the expression levels of the ER target genes *PDZK1*, *EGR3*, and *PGR* that increased in a very similar concentration range upon treatment with the reference substances as compared to the increase of the respective MI (Fig. 3B; Figure S3B). Notably, the expression levels of these ER target genes were only partially restored in BPA-treated cells, which correlated with its borderline MI_{max}. Furthermore, the two 'negative' reference substances Atra and Reserp did not have any effect on ER target gene expression at non-cytotoxic concentrations reinsuring that the slight increase in the MI in the presence of these substances was not reflecting estrogenic activity.

These results led to the development of a two-step data interpretation procedure describing a) acceptance criteria that define a valid run and flag cytotoxicity, and b) a classification model that provides the final prediction for a test substance (Fig. 4A). In the E-Morph Assay, each substance is, along with the solvent and Fulv controls, tested in 12 consecutive concentrations from 100 μM to 100 pM in technical triplicates allowing the simultaneous evaluation of two different substances on a single 96-well plate (see plate layout in File S3). The acceptance criteria include an assessment of the signal window for each test plate ($SW > 2.0$ or $Z' > 0.4$) as well as the exclusion of test wells from further analysis that show excessive cytotoxicity ($ToxN < 0.85$ or $ToxSI > 2.0$). A single run is considered positive (Pos) when the MI_{max} was above 0.75 in at least one of the tested non-cytotoxic concentrations. If that was not the case, the respective run is considered negative (Neg). The individual conclusions from three independent runs (biological triplicates) are combined to derive an overall binary classification by applying a '2-out-of-3' approach. Accordingly, a test substance is classified as positive (POS) or negative (NEG) when the MI_{max} was above or below 0.75 in at least two independent runs. Even if individual conclusions from the first two single runs were concordant (Pos or Neg), a third run would be recommended to evaluate the level of confidence of the overall classification. As for every other test method using cut-offs to define classification thresholds, experimental results close to the threshold are associated with a higher uncertainty. Borderline ranges around these thresholds that indicate ambiguous results were not yet considered in the E-Morph Assay, but can probably be statistically determined in the future when a larger number of substances has been tested and accepted guidance for the statistical method to be applied becomes available. In addition to the binary classification, the E-Morph Assay also enables an estimation of the potency of test substances by calculating the MI75, i.e. the interpolated concentration at which the MI equals 0.75 (see materials and methods). For test substances with sufficiently strong estrogenic activity, EC50 concentrations may be additionally calculated from MI dose-response curves as shown for the E2-titration in Fig. 1G-G′. The results from individual runs and the derived final binary classifications

Table 2
Binary classification and estimated potency of 17 chemicals tested in the E-Morph Assay.

Chemical name	CAS No.	Binary classification (MI_{max})					Estimated potency (logMI75)					Estimated potency (logEC50)					Estrogenic activity
		Run1	Run2	Run3	Overall	Confi-dence	Run1	Run2	Run3	Med	ER bioactivity	Run1	Run2	Run3	Med	ER bioactivity	
17β-Estradiol	50-28-2	Pos	Pos	Pos	POS	++	−8.36	−8.68	−8.82	−8.68	1.03	−8.63	−8.74	−8.77	−8.74	1.00	strong
17α-Ethinylestradiol	57-63-6	Pos	Pos	Pos	POS	++	−8.42	−8.86	−8.22	−8.42	1.00	−8.78	−8.92	−8.65	−8.78	1.00	strong
Diethylstilbestrol	56-53-1	Pos	Pos	Pos	POS	++	−8.09	−7.68	−8.18	−8.09	0.96	−8.30	−8.10	−8.31	−8.30	0.95	strong
Estrone	53-16-7	Pos	Pos	Pos	POS	++	−8.01	−7.99	−7.93	−7.99	0.95	−8.27	−7.50	−7.97	−7.97	0.91	strong
Coumestrol	479-13-0	Pos	Pos	Pos	POS	++	−7.02	−6.87	−6.65	−6.87	0.82	−6.94	−6.79	−6.83	−6.83	0.78	moderate
Zearalenone	17924-92-4	Pos	Pos	Pos	POS	++	−6.77	−6.51	−6.49	−6.51	0.77	−7.08	−6.67	−6.47	−6.67	0.76	moderate
Genistein	446-72-0	Pos	Pos	Pos	POS	++	−5.76	−6.84	−6.34	−6.34	0.75	−5.88	−6.86	−7.10	−6.86	0.78	moderate
5α-Dihydrotestesterone	521-18-6	Pos	Pos	Pos	POS	++	−5.02	−5.64	−6.82	−5.64	0.67	−5.25	−5.42	−5.89	−5.42	0.62	moderate
Daidzein	486-66-8	Pos	Pos	Pos	POS	++	−4.89	−5.52	−6.14	−5.52	0.65	−4.94	−5.52	−5.64	−5.52	0.63	moderate
Bisphenol AF	1478-61-1	Pos	Pos	Pos	POS	++	−6.37	−5.21	−5.27	−5.27	0.63	NA	NA	NA	NA	NA	moderate
Bisphenol S	80-09-1	Pos	Pos	Pos	POS	++	−4.51	−4.08	−4.48	−4.48	0.53	−4.60	−4.71	−4.77	−4.71	0.54	weak
Bisphenol B	77-40-7	Pos	Pos	Pos	POS	++	−4.52	−4.33	−4.35	−4.35	0.52	NA	NA	NA	NA	NA	weak
Bisphenol A	80-05-7	Pos	Pos	Neg	POS	+	−6.38	−4.38	Neg	−4.38	0.52	NA	NA	Neg	NA	NA	weak
Reserpine	50-55-5	Pos	Neg	Neg	NEG	+	−8.23	Neg	Neg	Neg	0.00	NA	Neg	Neg	Neg	0.00	negative
Progesterone	57-83-0	Neg	Neg	Pos	NEG	+	Neg	Neg	−5.81	Neg	0.00	Neg	Neg	NA	Neg	0.00	negative
Ketoconazole	65277-42-1	Neg	Neg	Pos	NEG	+	Neg	Neg	−5.38	Neg	0.00	Neg	Neg	NA	Neg	0.00	negative
Atrazine	1912-24-9	Pos	Neg	Neg	NEG	+	−4.36	Neg	Neg	Neg	0.00	NA	Neg	Neg	Neg	0.00	negative

Cells were exposed to 10 nM Fulv in combination with increasing concentrations of 17 reference chemicals for 48 h, stained, and analyzed using an image analysis pipeline. Each individual run was rated 'Pos' if the maximal MI (MImax) was greater than 0.75 at any tested concentration. The overall binary classification of each test chemical was derived using a '2-out-of-3' approach. The confidence of this classification is indicated based on the number of concordant conclusions from individual runs. Where applicable, the estimated potency of each test substance was calculated based on the interpolated log concentration at which the MI passed the 0.75 threshold (logMI75) or calculated from the dose-response curve (logEC50). The estimated potency of each test chemical was further ranked by normalization of its median logMI75 or median logEC50 value to 17α-Ethinylestradiol to derive an ER bioactivity score. Each run represents a biological replicate experiment. Med, median. NA, not applicable (no clear dose-response curve).

and estimated potencies of the six reference chemicals that were used for the development of the classification model are summarized in Table 2.

3.5. Proof-of-concept study

To evaluate the classification model and to assess its predictive capacity, we screened an additional set of 11 substances covering different chemical classes and diverse functions and activities (Table 1). This proof-of-concept study was performed according to the above-described E-Morph Assay set-up and data interpretation procedure (see materials and methods). The results from individual runs and the final binary classifications and estimated potencies of the 11 additional test substances are summarized in Table 2. Comparing these results with published reference data from regulatory accepted *in vivo* and *in vitro* test methods (Kleinstreuer et al. 2016; Laws and Wilson 2014; OECD 2012; 2015; 2016b) as well as screening data from the ToxCast project (Browne et al. 2015; Judson et al. 2015) showed that the binary classifications from the E-Morph Assay were fully concordant (Table 3). The E-Morph Assay correctly predicted 4/4 negative and 13/13 positive reference substances suggesting a similar predictive capacity in terms of sensitivity and specificity for the identification of hazardous substances as compared to the available test methods.

The estimated potencies were further converted into a relative ER bioactivity score by normalization of the median logMI75 and logEC50 values of each individual tested substance to the respective median of the potent estrogen EE (see materials and methods). This way, the relative ER bioactivity score allowed the grouping of the tested substances into four main categories of estrogenic activity, i.e. 'strong' (>0.9), 'moderate' (0.9–0.6), 'weak' (<0.6), and 'negative' (0.0) (Fig. 4B; Table 2). Among these substances, all estrogens occurring as natural hormones or used in pharmaceutical products were present in the 'strong' category. The 'moderate' category was mainly dominated by phytoestrogens, but notably, the androgen 5α-Dihydrotestosterone (DHT) and the industrial chemical Bisphenol AF (BPAF) were also in this category. The other tested bisphenols (Bisphenol S (BPS), Bisphenol B (BPB), and BPA) were categorized as 'weak' estrogenic substances. Reserp, Progesterone (PG), Ketoconazole (KetoC), and Atra were included in the 'negative' category.

In addition to grouping, the relative ER bioactivity score also facilitated direct comparisons of the estimated potencies of the test substances between the E-Morph Assay and existing ER test methods. Therefore, the available potency data from established *in vivo* [OECD TG 440] and *in vitro* [OECD TG 493, 455] test methods (OECD 2007; 2015; 2016b) were also normalized to EE (see materials and methods) (Table 3). The relative ER bioactivities of the substances that were tested in the E-Morph Assay correlated very well with these reference data and the ToxCast ER Agonist score (Fig. 4C) suggesting a comparable predictivity of the E-Morph Assay in terms of potency determination as compared to available test methods. Together, these data demonstrate the validity of the here-described classification model to identify and characterize substances with estrogenic activity in the E-Morph Assay.

4. Conclusion

The classification of chemicals as EDCs according to the WHO/IPCS definition (WHO/IPCS 2002) requires test methods that ideally provide information on endocrine modes-of-action and, at the same time, are predictive for endocrine-relevant adverse health effects in the whole organism. The results from the currently established mechanism-based *in vitro* test methods that address ER binding or transactivation (OECD 2015; 2016b) are not intended to be directly extrapolated to the complex signaling events and regulatory mechanisms that are present in an intact endocrine system *in vivo*. These assays rather provide useful information on possible mode-of-actions to establish a plausible link to adverse effects observed *in vivo*, which is required for classification of endocrine disruptors. The E-Morph Assay can moreover facilitate to establish a relevant mechanistic explanation for adverse *in vivo* effects as it is based on an intact, complete, and interconnected endogenous estrogen signaling pathway taking into account, e.g., EGFR signaling activity (Bischoff et al. 2020). By detecting both genomic (nuclear) and non-genomic (extra-nuclear) responses of cells to estrogens and anti-estrogens, the E-Morph Assay covers a broad effect spectrum of environmental chemicals with endocrine activity. In addition, it addresses the regulation of a clinically-relevant functional endpoint, i.e. AJ organization, in breast cancer cells (Bischoff et al. 2020) that is of central importance for tumor progression and metastasis. However, just like the great majority of available cell culture models and standardized test methods, the E-Morph Assay uses a cancer cell line instead of primary cells and therefore does not fully cover the diverse interactions and regulatory mechanisms of an intact *in vivo* system. As compared to co-culture or 3D cell culture models (Caron-Beaudoin et al. 2017; Deng et al. 2020; Hudon Thibeault et al. 2014; Marchese and Silva 2012; Speroni et al. 2014; Yancu et al. 2020), the E-Morph Assay provides less information with regard to potential effects of chemicals on breast tissue ductal structure or interaction between different cell types. Even though a simple assay set-up is generally advantageous for screening purpose, the informative value of the E-Morph Assay may benefit from integration of additional cell types in future studies.

The E-Morph Assay is the first test method that leverages the potential of high-content imaging and machine learning approaches to determine estrogenic activity based on morphological changes in a quantitative manner. In order to reflect human relevance, to the extent possible, the E-Morph Assay is performed under physiologically and clinically relevant cell culture conditions (see materials and methods). To ensure meaningful test results, it further integrates readouts to monitor cell viability and detect cytotoxicity, which is not always accounted for in other ER assays. Moreover, the E-Morph Assay is a valuable alternative to the existing luciferase-based ER transactivation assays (OECD 2016b), because it facilitates the testing of substances that might interfere with luciferase enzyme activity resulting in non-receptor-mediated luminescence as reported for phytoestrogens like Genistein or Resveratrol (Bakhtiarova et al. 2006; Sotoca et al. 2010). The possibility to screen for both ER agonistic and antagonistic effects of test substances using the same readout illustrates the versatility of the E-Morph Assay as, e.g., compared to existing ER binding assays (OECD 2015).

Due to its simple high-throughput compatible assay set-up and high concordance with available reference data, the E-Morph Assay appears to be fit-for-purpose to be integrated into ongoing EDC screening programs, such as those performed under the ToxCast project. It facilitates the rapid generation of concentration-response information to identify and precisely characterize substances that interact with the estrogen system. This way, it can particularly support the more comprehensive assessment of potential mixture effects of chemicals as recently described for EDCs with estrogenic activity (Schlotz et al. 2017; Yu et al. 2019). Follow-up screenings of larger compound libraries similar to the ToxCast project but based on independent peer-reviewed validation studies will further refine the applicability domain and predictive capacity of the E-Morph Assay.

In a regulatory context, specific Adverse Outcome Pathway (AOP)-based testing strategies that integrate data derived from a combination of multiple standardized test methods (e.g. *in vivo*, *in vitro*, *in silico*) can inform the chemical safety decision making process in the context of integrated approaches to testing and assessment (IATA) (OECD 2016a). Using an updated ToxCast ER model (Judson et al. 2017), the consideration of HTS assays in the context of an IATA for identification and assessment of ER active chemicals has recently been proposed (OECD 2019). The performance of the ToxCast ER model against curated *in vivo* reference data from the uterotrophic bioassay in rodents (Kleinstreuer et al. 2016; OECD 2007) even led to its consideration as an alternative for EDSP Tier 1 regulatory guideline studies addressing ER activity (US EPA 2015). The high level of concordance between E-Morph Assay

Table 3
Comparison of classifications from the E-Morph Assay with published reference data.

Chemical name	CAS No.	E-Morph Assay			Uterotrophic Assay (OECD TG 440)[a)]		Protein binding assays (OECD TG 493)[b)]					Transactivation assays (OECD TG 455)[e)]					Screening assays (U.S. EPA EDSP)
		Binary class	Median logMI75	ER bioactivity (rel.logMI75)	Binary class	Pos/Neg tests	Binary class[b-d)]	Freyberger-Wilson Assay		CERI Assay		Binary class[c),e)]	SSTA ER TA Assay		VM7-Luc-ER TA Assay		ToxCast ER Agonist Score[f)]
								logIC50[d)]	ER bioactivity (rel.logIC50)	logIC50[d)]	ER bioactivity (rel.logIC50)		logPC50[e)]	ER bioactivity (rel.logPC50)	logEC50[e)]	ER bioactivity (rel.logEC50)	
17β-Estradiol	50-28-2	POS	−8.68	1.03	POS	25/0	POS	−8.79	0.97	−8.92	1.05	POS	−11.00	1.00	−11.25	1.01	0.935
17α-Ethinylestradiol	57-63-6	POS	−8.42	1.00	POS	59/0	POS	−9.04	1.00	−8.47	1.00	POS	−11.00	1.00	−11.14	1.00	1.000
Diethylstilbestrol	56-53-1	POS	−8.09	0.96	POS	8/1	POS	−8.58	0.95	−8.04	0.95	POS	−10.69	0.97	−10.48	0.94	0.943
Estrone	53-16-7	POS	−7.99	0.95	POS	9/0	POS	–	–	–	–	POS	−9.23	0.84	−9.63	0.86	0.807
Coumestrol	479-13-0	POS	−6.87	0.82	–	–	POS	–	–	–	–	POS	−7.70	0.70	−6.88	0.62	–
Zearalenone	17924-92-4	POS	−6.51	0.77	POS	4/0	POS	−7.48	0.83	−6.99	0.83	POS	−9.19	0.84	–	–	0.710
Genistein	446-72-0	POS	−6.34	0.75	POS	27/1	POS	−6.88	0.76	−5.55	0.66	POS	−7.61	0.69	−6.57	0.59	0.538
5α-Dihydrotestesterone	521-18-6	POS	−5.64	0.67	POS	3/0	POS	−6.04	0.67	−8.04	0.95	POS	−6.28	0.57	–	–	0.400
Daidzein	486-66-8	POS	−5.52	0.65	EQUIV	1/1	POS	–	–	–	–	POS	−6.82	0.62	−6.10	0.55	0.440
Bisphenol AF	1478-61-1	POS	−5.27	0.63	POS	4/0	–	–	–	–	–	POS	−7.10	0.65	–	–	0.552
Bisphenol S	80-09-1	POS	−4.48	0.53	POS	2/0	–	–	–	–	–	–	–	–	–	–	0.263
Bisphenol B	77-40-7	POS	−4.35	0.52	POS	2/0	POS	–	–	–	–	POS	−6.68	0.61	−6.71	0.60	0.491
Bisphenol A	80-05-7	POS	−4.38	0.52	POS	37/6	POS	−5.98	0.66	−5.31	0.63	POS	−6.53	0.59	−6.27	0.56	0.450
Reserpine	50-55-5	NEG	Neg	0.00	EQUIV	1/1	NEG	–	–	–	–	NEG	Neg	0.00	Neg	0.00	0.000
Progesterone	57-83-0	NEG	Neg	0.00	–	–	NEG	Non-Binder	0.00	Non-Binder	0.00	–	–	–	–	–	0.051
Ketoconazole	65277-42-1	NEG	Neg	0.00	–	–	NEG	–	–	–	–	NEG	Neg	0.00	Neg	0.00	0.000
Atrazine	1912-24-9	NEG	Neg	0.00	NEG	0/2	NEG	Non-Binder	0.00	Non-Binder	0.00	NEG	Neg	0.00	Neg	0.00	0.000

The overall binary classifications and estimated potencies of 17 reference chemicals that were tested in the E-Morph Assay (see Table 2) were compared with published *in vivo* and *in vitro* reference data, and screening data from the ToxCast project. To facilitate a direct comparison of these data with the relative ER bioactivity that was measured in the E-Morph Assay, the published potencies from the individual assays were also normalized to 17α-Ethinylestradiol.

a) A Curated Database of Rodent Uterotrophic Bioactivity (Kleinstreuer et al., 2016).
b) Test No. 493: Performance-Based Test Guideline for Human Recombinant Estrogen Receptor (hrER) In Vitro Assays to Detect Chemicals with ER Binding Affinity (OECD, 2015).
c) Performance Standards For Stably Transfected Transactivation In Vitro Assay to Detect Estrogen Receptor Agonists for TG 455.
d) Integrated Summary Report: Validation of Two Binding Assays Using Human Recombinant Estrogen Receptor Alpha (hrERa) (Laws and Wilson, 2014).
e) Test No. 455: Performance-Based Test Guideline for Stably Transfected Transactivation In Vitro Assays to Detect Estrogen Receptor Agonists and Antagonists (OECD, 2016).
f) Screening Chemicals for Estrogen Receptor Bioactivity Using a Computational Model (Browne et al., 2015).

classifications and the ToxCast ER Agonist score imply that results from the E-Morph Assay can also be considered in testing strategies and IATAs to identify substances with endocrine disrupting properties and to prioritize substances or mixtures of concern for further testing. However, the demonstration of the reliability of the E-Morph Assay in terms of transferability and within-/between lab reproducibility will require larger ring trial studies involving naïve labs in the future. Such validation studies will be an important corner stone for a potential international acceptance of the E-Morph Assay for regulatory purpose. These studies will further ensure that the E-Morph Assay can significantly contribute to reducing the number of animals that are globally used for the testing of environmental chemicals and to eventually fully replace traditional *in vivo* studies, which yet still represent the gold standard with regard to the assessment of EDCs.

The E-Morph Assay addresses an important key event, i.e. the estrogen-dependent malignant transformation process of AJs, which among other pathological mechanisms can lead to breast cancer (Ye and Weinberg 2015). By studying the interconnected molecular mechanisms downstream of ER that regulate cell-cell contact morphology and stability in breast cancer cells, the E-Morph Assay could further support the development of more comprehensive AOPs for breast cancer (AOP 200, http://aopwiki.org/) that aim to achieve a complete overview of cancer susceptibility, initiation, progression, and metastasis (Ankley et al. 2010; Morgan et al. 2016; Vinken et al. 2017). Finally, the E-Morph Assay may also be used in the pharmaceutical sector for screening of novel active substances during the drug discovery process as well as for the development and testing of pharmaceutical compounds, e.g. for treatment of patients with estrogen-receptor positive breast cancer. Thus, the E-Morph Assay can support the development of therapy options as well as the identification of hazardous substances and might therefore play an important role at the interface of biomedical research and regulatory toxicology (Stolz et al. 2020).

CRediT authorship contribution statement

Marja Kornhuber: Conceptualization, Methodology, Data curation, Formal analysis, Software, Writing - original draft. **Sebastian Dunst:** Conceptualization, Supervision, Visualization, Writing - original draft. **Gilbert Schönfelder:** Funding acquisition, Writing - review & editing. **Michael Oelgeschäger:** Conceptualization, Supervision, Writing - review & editing.

Declaration of Competing Interest

The authors declare the following financial interests/personal relationships which may be considered as potential competing interests: A European (EP 3517967 A1) and international (PCT) (WO 2019145517 A1) patent application for the endpoint and conceptual design of the here-described E-Morph Assay to screen substances for estrogenic or anti-estrogenic activity has been filed at the European Patent Office by the employer (German Federal Institute for Risk Assessment (BfR)) of the authors. The German Federal Institute for Risk Assessment (BfR) is a scientifically independent institution within the portfolio of the Federal Ministry of Food and Agriculture (BMEL) in Germany. The authors' freedom to design, conduct, interpret, and publish research is explicitly not compromised.

Acknowledgements

We thank Ana Soto (Tufts University, USA) for providing the parental MCF-7/BOS cell line and colleagues from BfR/Bf3R for scientific input and comments on the manuscript. This work was supported by an internal BfR research funding program (Sonderforschungsprojekt 1322-683).

Appendix A. Supplementary material

Supplementary data to this article can be found online at https://doi.org/10.1016/j.envint.2021.106411.

References

Ankley, G.T., Bennett, R.S., Erickson, R.J., Hoff, D.J., Hornung, M.W., Johnson, R.D., Mount, D.R., Nichols, J.W., Russom, C.L., Schmieder, P.K., Serrrano, J.A., Tietge, J. E., Villeneuve, D.L., 2010. Adverse outcome pathways: a conceptual framework to support ecotoxicology research and risk assessment. Environ. Toxicol. Chem. 29 (3), 730–741.

Bakhtiarova, A., Taslimi, P., Elliman, S.J., Kosinski, P.A., Hubbard, B., Kavana, M., Kemp, D.M., 2006. Resveratrol inhibits firefly luciferase. Biochem. Biophys. Res. Commun. 351 (2), 481–484.

Benedetti, M., Zona, A., Beccaloni, E., Carere, M., Comba, P., 2017. Incidence of Breast, Prostate, Testicular, and Thyroid Cancer in Italian Contaminated Sites with Presence of Substances with Endocrine Disrupting Properties. Int. J. Environ. Res. Public Health 14.

Berx, G., van Roy, F., 2009. Involvement of members of the cadherin superfamily in cancer. Cold Spring Harb. Perspect. Biol. 1 (6), a003129.

Bischoff, P.; Kornhuber, M.; Dunst, S.; Zell, J.; Fauler, B.; Mielke, T.; Taubenberger, A.V.; Guck, J.; Oelgeschlager, M.; Schonfelder, G., 2020. Estrogens Determine Adherens Junction Organization and E-Cadherin Clustering in Breast Cancer Cells via Amphiregulin. iScience 23:101683.

Browne, P., Judson, R.S., Casey, W.M., Kleinstreuer, N.C., Thomas, R.S., 2015. Screening Chemicals for Estrogen Receptor Bioactivity Using a Computational Model. Environ. Sci. Technol. 49 (14), 8804–8814.

Caron-Beaudoin, E., Viau, R., Hudon-Thibeault, A.-A., Vaillancourt, C., Sanderson, J.T., 2017. The use of a unique co-culture model of fetoplacental steroidogenesis as a screening tool for endocrine disruptors: The effects of neonicotinoids on aromatase activity and hormone production. Toxicol. Appl. Pharmacol. 332, 15–24.

Carpenter, A.E., Jones, T.R., Lamprecht, M.R., Clarke, C., Kang, I.H., Friman, O., Guertin, D.A., Chang, J.H., Lindquist, R.A., Moffat, J., Golland, P., Sabatini, D.M., 2006. Cell Profiler: image analysis software for identifying and quantifying cell phenotypes. Genome Biol. 7, R100.

Deng, Y., Miki, Y., Nakanishi, A., 2020. Estradiol/GPER affects the integrity of mammary duct-like structures in vitro. Sci. Rep. 10, 1386.

Dix, D.J., Houck, K.A., Martin, M.T., Richard, A.M., Setzer, R.W., Kavlock, R.J., 2007. The ToxCast program for prioritizing toxicity testing of environmental chemicals. Toxicol. Sci. 95 (1), 5–12.

EC, 2006. Regulation (EC) No 1907/2006 of the European Parliament and of the Council of 18 December 2006 concerning the Registration, Evaluation, Authorisation and Restriction of Chemicals (REACH) (OJ L 396, 30.12.2006).

EC, 2009. Regulation (EC) No 1107/2009 of the European Parliament and of the Council of 21 October 2009 concerning the placing of plant protection products on the market (OJ L 309, 24.11.2009).

EC/BKH, 2000. Towards the establishment of a priority list of substances for further evaluation of their role in endocrine disruption - preparation of a candidate list of substances as a basis for priority setting.

EU, 2012. Regulation (EU) No 528/2012 of the European Parliament and of the Council of 22 May 2012 concerning the making available on the market and use of biocidal products (OJ L 167, 27.6.2012).

Fuentes, N., Silveyra, P., 2019. Estrogen receptor signaling mechanisms. Adv. Protein Chem. Struct. Biol. 116, 135–170.

Giulivo, M., Lopez de Alda, M., Capri, E., Barceló, D., 2016. Human exposure to endocrine disrupting compounds: Their role in reproductive systems, metabolic syndrome and breast cancer. A review. Environ. Res. 151, 251–264.

Hashizume, R., Koizumi, H., Ihara, A., Ohta, T., Uchikoshi, T., 1996. Expression of beta-catenin in normal breast tissue and breast carcinoma: a comparative study with epithelial cadherin and alpha-catenin. Histopathology 29, 139–146.

Hudon Thibeault, A.-A., Deroy, K., Vaillancourt, C., Sanderson, J.T., 2014. unique co-culture model for fundamental and applied studies of human fetoplacental steroidogenesis and interference by environmental chemicals. Environ. Health Perspect. 122 (4), 371–377.

Iversen, P.W.; Beck, B.; Chen, Y.-F.; Dere, W.; Devanarayan, V.; Eastwood, B.J.; Farmen, M.W.; Iturria, S.J.; Montrose, C.; Moore, R.A., 2012. HTS assay validation. Assay Guidance Manual [Internet]: Eli Lilly & Company and the National Center for Advancing Translational Sciences.

Johansson, H.K.L., Svingen, T., Fowler, P.A., Vinggaard, A.M., Boberg, J., 2017. Environmental influences on ovarian dysgenesis - developmental windows sensitive to chemical exposures. Nat. Rev. Endocrinol. 13 (7), 400–414.

Jones, T.R., Kang, I.n., Wheeler, D.B., Lindquist, R.A., Papallo, A., Sabatini, D.M., Golland, P., Carpenter, A.E., 2008. Cell Profiler Analyst: data exploration and analysis software for complex image-based screens. BMC Bioinf. 9 (1), 482. https://doi.org/10.1186/1471-2105-9-482.

Judson, R.S., Houck, K.A., Kavlock, R.J., Knudsen, T.B., Martin, M.T., Mortensen, H.M., Reif, D.M., Rotroff, D.M., Shah, I., Richard, A.M., Dix, D.J., 2010. In vitro screening of environmental chemicals for targeted testing prioritization: the ToxCast project. Environ. Health Perspect. 118 (4), 485–492.

Judson, R.S., Houck, K.A., Watt, E.D., Thomas, R.S., 2017. On selecting a minimal set of in vitro assays to reliably determine estrogen agonist activity. Regul. Toxicol. Pharm. 91, 39–49.

Judson, R.S., Magpantay, F.M., Chickarmane, V., Haskell, C., Tania, N., Taylor, J., Xia, M., Huang, R., Rotroff, D.M., Filer, D.L., Houck, K.A., Martin, M.T., Sipes, N., Richard, A.M., Mansouri, K., Setzer, R.W., Knudsen, T.B., Crofton, K.M., Thomas, R. S., 2015. Integrated Model of Chemical Perturbations of a Biological Pathway Using 18 In Vitro High-Throughput Screening Assays for the Estrogen Receptor. Toxicol. Sci. 148 (1), 137–154.

Kleinstreuer, N.C., Ceger, P.C., Allen, D.G., Strickland, J., Chang, X., Hamm, J.T., Casey, W.M., 2016. A Curated Database of Rodent Uterotrophic Bioactivity. Environ. Health Perspect. 124 (5), 556–562.

Kortenkamp, A., Martin, O., Faust, M., Evans, R., McKinlay, R., Orton, F., Rosivatz, E., 2011. State of the Art of the Assessment of Endocrine Disruptors. Final Report.

La Merrill, M.A., Vandenberg, L.N., Smith, M.T., Goodson, W., Browne, P., Patisaul, H.B., Guyton, K.Z., Kortenkamp, A., Cogliano, V.J., Woodruff, T.J., Rieswijk, L., Sone, H., Korach, K.S., Gore, A.C., Zeise, L., Zoeller, R.T., 2020. Consensus on the key characteristics of endocrine-disrupting chemicals as a basis for hazard identification. Nat. Rev. Endocrinol. 16 (1), 45–57.

Laws, S., Wilson, V., 2014. Integrated Summary Report: Validation of Two Binding Assays Using Human Recombinant Estrogen Receptor Alpha (hrERa). US Environ. Protect. Agency.

Marchese, S.; Silva, E., 2012. Disruption of 3D MCF-12A breast cell cultures by estrogens–an in vitro model for ER-mediated changes indicative of hormonal carcinogenesis. PLoS One 7:e45767.

McCormack, P., Sapunar, F., 2008. Pharmacokinetic profile of the fulvestrant loading dose regimen in postmenopausal women with hormone receptor-positive advanced breast cancer. Clin. Breast Cancer 8 (4), 347–351.

Morgan, M.M., Johnson, B.P., Livingston, M.K., Schuler, L.A., Alarid, E.T., Sung, K.E., Beebe, D.J., 2016. Personalized in vitro cancer models to predict therapeutic response: Challenges and a framework for improvement. Pharmacol. Ther. 165, 79–92.

OECD, 2001. Test No. 416: Two-Generation Reproduction Toxicity. OECD Publishing.

OECD, 2007. Test No. 440: Uterotrophic Bioassay in Rodents. OECD Publishing.

OECD, 2011. Test No. 456: H295R Steroidogenesis Assay edˆeds: OECD Publishing.

OECD, 2012. Performance Standards For Stably Transfected Transactivation In Vitro Assay to Detect Estrogen Receptor Agonists for TG 455. OECD Publishing.

OECD, 2015. Test No. 493: Performance-Based Test Guideline for Human Recombinant Estrogen Receptor (hrER) In Vitro Assays to Detect Chemicals with ER Binding Affinity. OECD Publishing.

OECD, 2016a. Guidance document for the use of adverse outcome pathways in developing integrated approaches to testing and assessment (IATA). OECD Publishing.

OECD, 2016b. Test No. 455: Performance-Based Test Guideline for Stably Transfected Transactivation In Vitro Assays to Detect Estrogen Receptor Agonists and Antagonists: OECD Publishing.

OECD, 2018a. Test No. 443: Extended One-Generation Reproductive Toxicity Study. OECD Publishing.

OECD, 2018b. Test No. 451: Carcinogenicity Studies. OECD Publishing.

OECD, 2018c. Test No. 452: Chronic Toxicity Studies. OECD Publishing.

OECD, 2018d. Test No. 453: Combined Chronic Toxicity/Carcinogenicity Studies. OECD Publishing.

OECD, 2019. Case Study on the Use of an Integrated Approach to Testing and Assessment for Identifying Estrogen Receptor Active Chemicals. OECD Publishing.

Qureshi, H.S., Linden, M.D., Divine, G., Raju, U.B., 2006. E-cadherin status in breast cancer correlates with histologic type but does not correlate with established prognostic parameters. Am. J. Clin. Pathol. 125 (3), 377–385.

Reif, D.M., Martin, M.T., Tan, S.W., Houck, K.A., Judson, R.S., Richard, A.M., Knudsen, T.B., Dix, D.J., Kavlock, R.J., 2010. Endocrine profiling and prioritization of environmental chemicals using ToxCast data. Environ. Health Perspect. 118 (12), 1714–1720.

Riss, T.; Niles, A.; Moravec, R.; Karassina, N.; Vidugiriene, J. Cytotoxicity Assays: In Vitro Methods to Measure Dead Cells. in: Sittampalam G.S., Grossman A., Brimacombe K., Arkin M., Auld D., Austin C.P., Baell J., Bejcek B., Caaveiro J.M.M., Chung T.D.Y., Coussens N.P., Dahlin J.L., Devanaryan V., Foley T.L., Glicksman M., Hall M.D., Haas J.V., Hoare S.R.J., Inglese J., Iversen P.W., Kahl S.D., Kales S.C., Kirshner S., Lal-Nag M., Li Z., McGee J., McManus O., Riss T., Saradjian P., Trask O.J., Jr., Weidner J.R., Wildey M.J., Xia M., Xu X. (Eds.), 2004. Assay Guidance Manual. Bethesda (MD).

Rothman, M.S., Carlson, N.E., Xu, M., Wang, C., Swerdloff, R., Lee, P., Goh, V.H.H., Ridgway, E.C., Wierman, M.E., 2011. Reexamination of testosterone, dihydrotestosterone, estradiol and estrone levels across the menstrual cycle and in postmenopausal women measured by liquid chromatography-tandem mass spectrometry. Steroids 76 (1-2), 177–182.

Rotroff, D.M., Dix, D.J., Houck, K.A., Knudsen, T.B., Martin, M.T., McLaurin, K.W., Reif, D.M., Crofton, K.M., Singh, A.V., Xia, M., Huang, R., Judson, R.S., 2013. Using in vitro high throughput screening assays to identify potential endocrine-disrupting chemicals. Environ. Health Perspect. 121 (1), 7–14.

Schlotz, N., Kim, G.-J., Jäger, S., Günther, S., Lamy, E., 2017. In vitro observations and in silico predictions of xenoestrogen mixture effects in T47D-based receptor transactivation and proliferation assays. Toxicol. In Vitro 45, 146–157.

Soto, A.M., Sonnenschein, C., 1985. The role of estrogens on the proliferation of human breast tumor cells (MCF-7). J. Steroid Biochem. 23 (1), 87–94.

Sotoca, A.M., Bovee, T.F.H., Brand, W., Velikova, N., Boeren, S., Murk, A.J., Vervoort, J., Rietjens, I.M.C.M., 2010. Superinduction of estrogen receptor mediated gene expression in luciferase based reporter gene assays is mediated by a post-transcriptional mechanism. J. Steroid Biochem. Mol. Biol. 122 (4), 204–211.

Speroni, L., Sweeney, M.F., Sonnenschein, C., Soto, A.M., 2016. A Hormone-responsive 3D Culture Model of the Human Mammary Gland Epithelium. J. Vis. Exp. (108), e53098. https://doi.org/10.3791/53098.

Speroni, L., Whitt, G.S., Xylas, J., Quinn, K.P., Jondeau-Cabaton, A., Barnes, C., Georgakoudi, I., Sonnenschein, C., Soto, A.M., 2014. Hormonal regulation of epithelial organization in a three-dimensional breast tissue culture model. Tissue Eng. Part C Methods 20 (1), 42–51.

Stolz, A., Becker, M., Wistorf, E., Ertych, N., 2020. Biomedical Research Meets Toxicology: How In Vitro Chromosome Instability Methods Can Contribute to Carcinogenicity Prediction. Cancer Res. 80 (8), 1626–1629.

US EPA, 2015. Use of High Throughput Assays and Computational Tools; Endocrine Disruptor Screening Program; Notice of Availability and Opportunity for Comment.

Villalobos, M., Olea, N., Brotons, J.A., Olea-Serrano, M.F., Ruiz de Almodovar, J.M., Pedraza, V., 1995. The E-screen assay: a comparison of different MCF7 cell stocks. Environ. Health Perspect. 103 (9), 844–850.

Vinken, M., Knapen, D., Vergauwen, L., Hengstler, J.G., Angrish, M., Whelan, M., 2017. Adverse outcome pathways: a concise introduction for toxicologists. Arch. Toxicol. 91 (11), 3697–3707.

Wakeling, A.E., Dukes, M., Bowler, J., 1991. A potent specific pure antiestrogen with clinical potential. Cancer Res. 51, 3867–3873.

Warth, B., Palermo, A., Rattray, N.J.W., Lee, N.V., Zhu, Z., Hoang, L.T., Cai, Y., Mazurek, A., Dann, S., VanArsdale, T., Fantin, V.R., Shields, D., Siuzdak, G., Johnson, C.H., 2019. Palbociclib and Fulvestrant Act in Synergy to Modulate Central Carbon Metabolism in Breast Cancer Cells. Metabolites 9 (1), 7. https://doi.org/10.3390/metabo9010007.

WHO/IPCS, 2002. IPCS global assessment of the state-of-the-science of endocrine disruptors. WHO/PCS/EDC/022, 35-50.

WHO/UNEP, 2013. State of the science of endocrine disrupting chemicals – 2012.

Wild, C.P.; Weiderpass, E.; Stewart, B.W. (Eds.), 2020. World Cancer Report: Cancer Research for Cancer Prevention edˆeds. Lyon, France: International Agency for Research on Cancer. Available from: http://publications.iarc.fr/586. Licence: CC BY-NC-ND 3.0 IGO.

Yager, J.D., Davidson, N.E., 2006. Estrogen carcinogenesis in breast cancer. N. Engl. J. Med. 354 (3), 270–282.

Yancu, D., Viau, R., Sanderson, T., 2020. Development of an estrogen-dependent breast cancer co-culture model as a tool for studying endocrine disruptors. Toxicol. In Vitro 62, 104658. https://doi.org/10.1016/j.tiv.2019.104658.

Ye, X., Weinberg, R.A., 2015. Epithelial-Mesenchymal Plasticity: A Central Regulator of Cancer Progression. Trends Cell Biol. 25 (11), 675–686.

Yu, H., Caldwell, D.J., Suri, R.P., 2019. In vitro estrogenic activity of representative endocrine disrupting chemicals mixtures at environmentally relevant concentrations. Chemosphere 215, 396–403.